

PARAMETER ESTIMATION FOR WIRELESS FADING AND TURBULENCE CHANNELS

by

NING WANG

B.Eng., Tianjin University, China, 2004

A THESIS SUBMITTED IN PARTIAL FULFILLMENT OF
THE REQUIREMENTS FOR THE DEGREE OF

MASTER OF APPLIED SCIENCE

in

The College of Graduate Studies

(Electrical Engineering)

THE UNIVERSITY OF BRITISH COLUMBIA
(OKANAGAN)

June 2010

© Ning Wang, 2010

Abstract

In this thesis, we mainly investigate the parameter estimation problem for fading and atmospheric turbulence channel models for wireless communications. A generalized method of moments (GMM) estimation scheme is introduced to the estimation of Nakagami fading parameter. Our simulation results and asymptotic performance analysis reveal that this GMM framework achieves the best performance among all method of moments estimators based on the same moment conditions. Further improved performance can be achieved using additional moment conditions in the GMM. In the study of the maximum-likelihood (ML) based Nakagami m parameter estimators, we observe that a parameter Δ , which is defined as the logarithmic ratio of the arithmetic mean to the geometric mean of the Nakagami- m fading power, can be used to assess the estimation performance of ML-based estimators analytically. For small sample size, the probability density function (PDF) of Δ is derived by the moment generating function (MGF) method. For large sample size scenarios, we use a moment matching method to approximate the PDF of Δ by a two-parameter Gamma PDF. This approximation is validated by the Kolmogorov-Smirnov (K-S) test as well as simulation results. When studying the Gamma-Gamma turbulence model for free-space optical (FSO) communication, an estimation scheme for the shape parameters of the Gamma-Gamma distribution is introduced based on the concept of fractional moments and convex optimization. A modified estimation scheme, which exploits the relationship between the Gamma-Gamma shape parameters in FSO communication, is also proposed. Simulation results show that this modified scheme can achieve satisfactory estimation performance over a wide range of turbulence conditions.

Table of Contents

Abstract	ii
Table of Contents	iii
List of Tables	vi
List of Figures	vii
List of Acronyms	ix
Acknowledgments	xi
1 Introduction	1
1.1 Background and Motivation	1
1.2 Fading and Turbulence Models for Wireless Communication	2
1.2.1 Multipath Fading Models	2
1.2.2 Atmospheric Turbulence Models	6
1.3 Moment-Based Estimation Techniques	7
1.4 Thesis Outline and Contributions	8
2 Moment-Based Estimation for the Nakagami-m Fading Parameter	10
2.1 Background and Motivation	10
2.2 Moment-Based m Parameter Estimation with Integer and Fractional Moments	11
2.2.1 Integer-Moment-Based m parameter Estimators	11

2.2.2	A Family of Fractional Moment-Based m Parameter Estimators	13
2.2.3	Large Sample Properties: Asymptotic Variance Analysis	15
2.3	Generalized Method of Moments Estimation	16
2.3.1	GMM Estimation for the Nakagami m Parameter	16
2.3.2	Derivation for Asymptotic Variance of the GMM Estimator	19
2.4	Numerical Results and Discussion	23
2.5	Summary	27
3	On Statistics of Logarithmic Ratio of Arithmetic Mean to Geometric Mean for Nakagami-m Fading Power	28
3.1	ML-Based Nakagami- m Parameter Estimators	28
3.2	Statistical Properties of Δ	30
3.2.1	Alternative Expression of Δ	30
3.2.2	Nonnegative Property of Δ	30
3.2.3	Moment Generating Function of Δ	31
3.2.4	Probability Density Function of Δ	32
3.3	Gamma Approximation	36
3.3.1	Gamma Approximation for PDF of Δ	36
3.3.2	Validating the Gamma Approximation	37
3.4	Applications and Numerical Results	41
3.5	Summary	44
4	Moment-Based Estimation for the Gamma-Gamma Distribution with FSO Applications	45
4.1	Introduction	45
4.2	Statistical Properties of the Gamma-Gamma Turbulence Model	47
4.2.1	Parameterization of the Gamma-Gamma Turbulence Model	47
4.2.2	Moments of The Gamma-Gamma Turbulence Model	49

Table of Contents

4.3	An <i>MoM/CVX</i> Estimation Scheme for Gamma-Gamma Shape Parameters . . .	51
4.4	A Modified <i>MoM/CVX</i> Estimation Scheme for the Shape Parameter α	55
4.5	Summary	57
5	Conclusions	59
5.1	Summary of Contributions	59
5.2	Future work	60
	Bibliography	62
 Appendices		
A	Derivation of (2.28)	67
B	Exponential Family Property of the Nakagami-m Distribution	69

List of Tables

3.1	Kolmogorov-Smirnov test for goodness-of-fit for the Gamma approximation. .	40
3.2	Numerical MSE performance evaluations for ML-based Nakagami m parameter estimators.	41

List of Figures

2.1	Simulated MSE performance of moment-based Nakagami fading parameter estimators with sample size $N = 10,000$	25
2.2	Asymptotic relative estimation efficiencies of moment-based Nakagami fading parameter estimators with respect to ML.	26
3.1	Comparison of empirical PDFs and analytical PDFs of Δ for $m = 0.5, 1, 2$ with sample size $N = 5$	34
3.2	Comparison of empirical PDFs and analytical PDFs of Δ for $m = 0.5, 1, 2$ with sample size $N = 10$	35
3.3	Comparison of empirical PDFs and Gamma approximated PDFs of Δ for $m = 0.5, 1, 2$ with sample size $N = 10$	38
3.4	Comparison of empirical PDFs and Gamma approximated PDFs of Δ for $m = 0.5, 1, 2$ with sample size $N = 100$	39
3.5	Analytical and simulated MSE performance of ML-based Nakagami m parameter estimators with sample size $N = 100$	43
4.1	Gamma-Gamma shape parameters α and β as functions of σ_R	48
4.2	Gamma-Gamma PDFs with Rytov variance $\sigma_R^2 = 0.25, 2, \text{ and } 11$	50
4.3	MSE performance of the <i>MoM/CVX</i> estimator and the modified <i>MoM/CVX</i> estimator with $k = 0.5$ and sample size $N = 100,000$	54
4.4	Absolute derivative functions of the Gamma-Gamma shape parameters α and β with respect to σ_R	56

List of Figures

4.5	Flow chart of the modified <i>MoM/CVX</i> estimator for the Gamma-Gamma shape parameters.	58
-----	---	----

List of Acronyms

Acronyms	Definitions
AF	Amount of Fading
CDF	Cumulative Distribution Function
CLT	Central Limit Theorem
CRLB	Cramer-Rao Lower Bound
FSO	Free-Space Optical
GDE	Greenwood-Durand Estimator
GMM	Generalized Method of Moments
INV	Inverse Normalized Variance
K-S	Kolmogorov-Smirnov
LOS	Line-of-Sight
LS	Least Squares
MGF	Moment Generating Function
FFT	Fast Fourier Transform
ML	Maximum-Likelihood
MLE	Maximum-Likelihood Estimator
MoM	Method of Moments
MoM/CVX	Method of Moments/Convex Optimization
MSE	Mean Square Error
MVUE	Minimum Variance Unbiased Estimator
PDF	Probability Density Function

List of Acronyms

RF	Radio Frequency
RV	Random Variable
WLLN	Weak Law of Large Numbers

Acknowledgments

Firstly and foremost, I would like to take this chance to give my warm and grateful thanks to my supervisor, Dr. Julian Cheng, for providing me with the opportunity to work in the field of wireless communication, and for his continuous support, encouragement, and guidance throughout my master's study.

I am deeply indebted to Dr. Richard Klukas and Dr. Stephen O'Leary for their great effort and significant amount of time to serve on my M.A.Sc. committee. I would also like to express my thanks to Dr. Shawn Wang from UBC Okanagan Mathematics and Statistics Department for both his help on my coursework and his willingness to serve as my external examiner. I really appreciate their valuable time and constructive comments on my thesis. In addition, I would like to thank Dr. Chintha Tellambura from University of Alberta for his feedback and valuable suggestions on my research work.

My thanks to all my labmates and friends at UBC Okanagan for their help and friendship. Special thanks to Xian Jin, Chiun-Shen Liao, Mingbo Niu, and Xuegui Song for always being available for technical discussions and for sharing their academic experiences generously.

Finally, I would like to express my deepest gratitude for the constant support, understanding and unconditional love that I received from my family.

Chapter 1

Introduction

1.1 Background and Motivation

With the capability of providing globally interconnected voice and data communication systems, as well as establishing local communication architecture for the interconnection of electronic devices, wireless communication is undoubtedly one of the most vibrant areas in communication theory research today. Modern wireless communication dates back to the invention of wireless telegraph system by Guglielmo Marconi over one hundred years ago. However, even though it emerged only 20 years after the invention of the telephone by Alexander Graham Bell, wireless communication was not widely used in the consumer communication market until the early 1980s. For nearly one century's time in the modern telecommunication history, most of the market was dominated by wireline communication.

Technologically, what impeded wireless communication from extensive application were the undesirable features of the wireless transmission environment. Being an open transmission medium, wireless channels can bring much more attenuation and uncertainty to the transmitted signal than wireline does, thus more sophisticated technologies have to be implemented in wireless systems to combat this disadvantage. Generally speaking, there are two fundamental challenges that have to be addressed for wireless communication. The first challenge is the random fluctuation of the transmitted signal. In radio frequency (RF) wireless communication systems, this is known as fading which is mainly due to the multipath effect and shadowing; whereas for a more recent line-of-sight (LOS) wireless communication technology, the free-space optical (FSO) communication, much smaller wavelength and directionality determine

that signal fluctuation in FSO is dominated by the effect of atmospheric turbulence but not fading. The second challenge for wireless communication is the interference from other users or other communication systems. Unlike wireline communication which uses a bounded transmission medium, communication through a wireless channel is more subject to interference because different users and different systems are sharing the same transmission medium. In this thesis, we address the first challenge and focus our study to the problem of parameter estimation for wireless fading and turbulence channel models. Knowledge of these parameter values can be used, for example, to design a better transmission scheme adaptive to the wireless links and to better characterize wireless channels for link budget analysis.

1.2 Fading and Turbulence Models for Wireless Communication

To address the first challenge for wireless communication, the random fluctuations of the transmitted signal, fading and atmospheric turbulence models are proposed for different application scenarios and channel conditions based on statistical study of received signals. However, modelling the pattern of the signal fluctuations is just the first step. In order to employ a fading or turbulence model in system design and performance analysis, it is also critical to determine or estimate the parameters of the model, which will fit the model to the specific channel conditions. This estimation process is what we will mainly discuss in this thesis. Before discussing the parameter estimation problem further, we will first review some well-known fading and turbulence models for wireless communications.

1.2.1 Multipath Fading Models

As a result of the random propagation (reflection, diffraction and scattering etc.) of radio waves in the wireless transmission environment, several replicas of the transmitted signal, with

different amplitudes and phases, arrive at the receiver end. When these signal replicas are not resolvable, they are added up constructively or destructively at the receiver, causing multipath fading or fading in short.

The delay spread, denoted by T_d , is one of the most important channel properties; it characterizes the time domain dispersive nature of the fading channel. In brief, T_d describes the arrival time span of all the available signal replicas. The reciprocal of T_d is known as the coherent bandwidth, which is denoted by W_c . When the signal bandwidth W is much smaller than W_c , the channel is considered as frequency-nonselctive or flat, which means that all the frequency components of the transmitted signal experience the same attenuation and phase shift. Otherwise, the channel is considered as frequency-selective fading.

Another important parameter which characterizes the frequency dispersive nature of the fading channel is the Doppler spread D_s ; the reciprocal of D_s is the coherent time T_c . When T_c is much larger than the delay requirement of the system, which is usually set to be the symbol duration T , the channel is considered to be a fast fading channel; otherwise the channel is said to be slow.

Therefore, based on the relative relation between properties of the transmitted signal (symbol duration T in time domain and signal bandwidth W in frequency domain) and properties of the wireless fading channel (coherent time T_c in time domain and coherent bandwidth W_c in frequency domain), we can classify fading channels into four basic types: fast frequency-selective fading, fast frequency-nonselctive fading, slow frequency-selective fading, and slow frequency-nonselctive fading. In this thesis, we focus on estimation of slow frequency-nonselctive fading models.

Regardless of noise and interference, the slow frequency-nonselctive fading channel can be described by the following expression

$$s_r(t) = \alpha \cdot s_t(t) \tag{1.1}$$

where $s_t(t)$ and $s_r(t)$ are transmitted and received complex signals respectively, and the complex random variable α represents the fading channel characteristics.

The first-order statistics of the fading channel, which characterizes the fading envelope or amplitude of the parameter α , is the most widely used approach to study fading effect. Among all the statistical models proposed for the fading envelope, the most well-known ones are Rayleigh, Rician, and Nakagami- m models.

The Rayleigh and Rician fading models are derived from Clarke's one-ring model [1] for the electromagnetic field of the received multipath signal. The Clarke's model assumes that between the transmitter and the receiver, there are N unresolvable paths with random amplitudes and phases. If no LOS path exists, for sufficiently large N , by the central limit theorem (CLT), all independent paths will have Gaussian distributed amplitudes and uniform phases. Therefore the real and imaginary parts of the sum will be independent and identically-distributed (i.i.d.) zero mean Gaussian RVs, and the corresponding fading envelope R will have a Rayleigh distribution with probability density function (PDF)

$$f_R(r) = \frac{2r}{\Omega} e^{-\frac{r^2}{\Omega}}, \quad r \geq 0 \quad (1.2)$$

where the parameter Ω is the fading power $\Omega = \mathbb{E}[R^2]$. When an LOS or specular path with known amplitude exists between the transmitter and the receiver, the real part and the imaginary part of the combined signal will be correlated, and the fading envelope will have a Rician distribution. The PDF of the Rician distribution is given by

$$f_R(r) = \frac{2r(\mathcal{K} + 1)}{\Omega} \exp\left\{-\mathcal{K} - \frac{(\mathcal{K} + 1)r^2}{\Omega}\right\} I_0\left(2r\sqrt{\frac{\mathcal{K}(\mathcal{K} + 1)}{\Omega}}\right), \quad r \geq 0 \quad (1.3)$$

where $I_0(\cdot)$ is the zeroth order modified Bessel function of the first kind, and the parameter \mathcal{K} is known as Rician K -factor which is defined as the ratio of the power in the specular path to the power in the scattered paths. According to the definition, the Rician K -factor indicates the

relative strength of the LOS component: when $\mathcal{K} = 0$, the LOS component disappears, and the Rician distribution specializes to Rayleigh distribution; when \mathcal{K} approaches infinity, the scattering components in the signal are negligible, and the channel becomes static or deterministic.

Different from the Rayleigh and Rician distributions, the Nakagami- m distribution was not derived from any theoretical model. It was originally deduced from experimental data [2]. Thus for a variety of fading conditions, the Nakagami- m model can fit the practical multipath fading measurements better than the other models. The PDF of the Nakagami- m distributed fading envelope is given by

$$f_R(r) = \frac{2}{\Gamma(m)} \left(\frac{m}{\Omega}\right)^m r^{2m-1} \exp\left(-\frac{m}{\Omega}r^2\right), \quad r \geq 0, m \geq \frac{1}{2} \quad (1.4)$$

where m is known as the fading parameter whose reciprocal quantifies the degree of fading, and $\Gamma(\cdot)$ is the Gamma function defined by

$$\Gamma(z) = \int_0^{+\infty} t^{z-1} e^{-t} dt. \quad (1.5)$$

The Nakagami- m distribution covers a wide range of fading conditions. It can be shown that when $m = \frac{1}{2}$, which corresponds to the most severe fading condition, the Nakagami- m distribution becomes the one-sided Gaussian distribution. The Rayleigh distribution can also be found as a special case of the Nakagami- m distribution by letting $m = 1$. Being capable of modelling a wide range of fading conditions as well as having a tractable PDF, the Nakagami- m fading model is a popular and widely used fading model in wireless communication research. Estimation of the Nakagami- m fading model is thus of great interest in wireless communications research.

1.2.2 Atmospheric Turbulence Models

As a typical LOS communication technology, FSO differs from most RF systems which suffer from fading due to multipath propagation. In FSO communication, the main impairment is caused by atmospheric turbulence-induced fluctuations [3]. Therefore, multipath fading models are no longer applicable to system design and performance analysis for FSO systems. Instead we focus on the study of atmospheric turbulence models.

For weak turbulence conditions, Parry [4] and Phillips and Andrews [5] independently suggested a log-normal PDF to model the irradiance, which is the power density of the optical beam. With unit mean irradiance and scintillation index σ_I^2 , the log-normal PDF of the irradiance I is given by [3]

$$f_L(I) = \frac{1}{I\sqrt{2\pi\sigma_I^2}} \exp\left\{-\frac{[\ln I + \frac{1}{2}\sigma_I^2]^2}{2\sigma_I^2}\right\}, \quad I > 0. \quad (1.6)$$

When turbulence becomes stronger, the negative exponential distribution was introduced as a limit distribution for the irradiance. This limit distribution can only provide sufficient accuracy when the system goes far into the saturation regime [6]. The K -distribution, which is based on an assumed modulation process, was later introduced to model the irradiance in strong turbulence scenarios [7]. The K -distribution with unit mean irradiance is characterized by the PDF [3]

$$f_K(I) = \frac{2\alpha}{\Gamma(\alpha)} (\alpha I)^{(\alpha-1)/2} K_{\alpha-1}(2\sqrt{\alpha I}), \quad I > 0 \quad (1.7)$$

where α is a positive shape parameter related to the effective number of discrete scatterers and $K_\nu(\cdot)$ is the ν th order modified Bessel function of the second kind.

Being a widely accepted turbulence model for FSO communication under strong turbulence conditions, the K -distribution is, however, incapable of modeling the irradiance when turbulence is weak. This is because the scintillation index given by the K distributed irradiance is always greater than unity, which is not valid for weak turbulence scenarios. Another

modulation-based model, the Gamma-Gamma distribution, was later proposed by Al-Habash *et al.* [8] to model the irradiance in FSO systems. The PDF of the Gamma-Gamma distribution is given by

$$f_G(I) = \frac{2(\alpha\beta)^{(\alpha+\beta)/2}}{\Gamma(\alpha)\Gamma(\beta)} I^{\frac{\alpha+\beta}{2}-1} K_{\alpha-\beta} \left(2\sqrt{\alpha\beta I} \right), \quad \alpha > 0, \beta > 0 \quad (1.8)$$

where α and β are the shape parameters. Note that by setting the shape parameter $\beta = 1$, the Gamma-Gamma distribution will degenerate to the K -distribution. The Gamma-Gamma turbulence model is desirable because for both weak and strong turbulence scenarios, this model can provide a good fit to the experimental measurements of irradiance [8]. Thus, the key advantage of using the Gamma-Gamma turbulence model is that it covers a wide-range of turbulence conditions.

1.3 Moment-Based Estimation Techniques

A number of statistical signal processing approaches have been introduced to parameter estimation in wireless communication research, among which the most popular ones in practical applications are the ML estimation and the method of moments (MoM) or the moment-based approach. Because of its asymptotic efficiency, the maximum likelihood estimator (MLE) is approximately the minimum variance unbiased estimator (MVUE) and the ML approach can also give us the Cramér-Rao lower bound (CRLB) for the MVUE which describes the best achievable estimation performance for unbiased estimators [9]. Therefore the ML approach is usually the more preferable one for theoretical studies. However, when the model, or more specifically the PDF of the fading or atmospheric turbulence that will be intensively discussed in this thesis, involves transcendental functions, the ML approach will likely involve solving an nonlinear transcendental equation or equation set, which can be undesirable in practice.

As an alternative approach, the method of moments can usually lead to estimators which are

easy to determine and implement [9]. Even though there exists no optimality properties for the moment-based approach, it can usually give satisfactory estimates when the sample size is large enough. The basic principle of the method of moments is to equate the population moments of the model to their sample counterparts. Several estimation techniques under the basic framework of MoM have been proposed by researchers. The most widely used one is the classical method of moments, which solves for unknown parameters in an equation or equation set derived from the moment conditions of the model. The generalized method of moments (GMM) approach [10] proposed a regression estimation scheme for determined and over-determined problems. Using linear combinations of order statistics, the L-moment method, a more robust method that suffers less from sampling variability, was introduced for estimation of distributions [11]. In addition, combinations of the moment-based approach and other estimation approaches are also reported [12] [13] [14]. Multiple moment-based estimation methods as well as combinations of estimation methods will be used in this thesis.

1.4 Thesis Outline and Contributions

This thesis have been divided into five chapters. Chapter 1 reviews some background knowledge about fundamental challenges for wireless communication: random fluctuation of the transmitted signal and the interference problem. To address the signal fluctuation problem, we first need to model the fluctuation pattern and then estimate corresponding characteristic parameters when applying the model in system design and performance analysis for specific application scenarios. This motivates researchers to find better estimators for popular fading and atmospheric turbulence models. It is pointed out that the method of moments is sometimes a preferable approach to ML when the model takes an intractable form.

In Chapter 2, we provide a detailed discussion on moment-based estimation for the Nakagami- m fading model. Firstly a family of classical moment-based m parameter estimators is reviewed, both integer moments scenario and fractional moments scenario are discussed. Then

the GMM method which exploits information resides in all moment conditions in a determined or over-determined estimation problem is introduced to fading parameter estimation for the first time. At last, a systematic performance comparison for moment-based m parameter estimators is conducted by both the simulated mean square error approach and the analytical asymptotic variance approach.

In Chapter 3, we use moment-based method to study performance of ML-based Nakagami m parameter estimators. By examining the derivation of the ML-based m parameter estimation problem, it is found that a parameter Δ , which is defined as the logarithmic ratio of arithmetic mean to geometric mean for Nakagami- m fading power, is critical to the ML-based m parameter estimation. Closed-form expressions are derived for the moment generating function (MGF) and the PDF of Δ . For large sample size, we use a moment matching method to approximate the PDF of Δ by a two-parameter Gamma PDF. This approximation is validated by the Kolmogorov-Smirnov (K-S) test. As an application, the approximate PDF is used to study the performance of three well known ML-based Nakagami m parameter estimators, the Greenwood-Durand estimator [15] and the first and second order Cheng-Beaulieu estimators [16].

Chapter 4 studies the parameter estimation of the Gamma-Gamma turbulence model for FSO communication. A novel estimation scheme for the shape parameters of the Gamma-Gamma distribution is proposed based on a combination of fractional MoM estimation and convex optimization. Then a modified estimation scheme, which turns out to be an improved one, is proposed by considering relationship between the Gamma-Gamma shape parameters for FSO applications. Revealed by computer simulation results, the modified scheme can achieve improved performance over a wide range of turbulence conditions.

Chapter 5 summarizes contents and contributions of this thesis, and suggests some possible future works in related topics.

Chapter 2

Moment-Based Estimation for the Nakagami- m Fading Parameter

2.1 Background and Motivation

The Nakagami- m fading model is important in wireless communications research because it fits the empirical multipath fading measurements better than the other fading models for a variety of fading conditions [2]. The Nakagami- m model is also desirable because error rate performance analysis with Nakagami fading often leads to closed-form analytical results.

The PDF of the Nakagami- m fading envelope R has a two-parameter form, which is given by [2]

$$f_R(r) = \frac{2}{\Gamma(m)} \left(\frac{m}{\Omega}\right)^m r^{2m-1} \exp\left(-\frac{m}{\Omega}r^2\right), \quad r \geq 0, m \geq \frac{1}{2} \quad (2.1)$$

where $\Omega = \mathbb{E}[R^2]$, and the fading parameter m is defined as [2]

$$m = \frac{\Omega^2}{\mathbb{E}[(R^2 - \Omega)^2]}, \quad m \geq \frac{1}{2}. \quad (2.2)$$

Given N independent realizations of the Nakagami- m random variable R_1, R_2, \dots, R_N , since the parameter Ω is defined as the second-order moment of the Nakagami- m fading envelope, it is straightforward to use the second order sample moment of the fading envelope to estimate Ω , which is $\hat{\Omega} = \hat{\mu}_2 = \frac{1}{N} \sum_{i=1}^N R_i^2$. Thus in order to characterize wireless communication channels using the Nakagami model, it is critical to determine or estimate the value of m , which is

also known as reciprocal of the amount of fading (AF), from N independent observations. Notice that the squared value of a Nakagami- m distributed random variable is a Gamma random variable, Nakagami m parameter estimation is sometimes related to estimation for the Gamma distribution.

Greenwood and Durand demonstrated that the ML-based m parameter estimation problem leads to solving a non-linear transcendental equation involving a natural logarithmic function and a digamma function [15]. The most well-known ML-based m parameter estimators, the Greenwood-Durand estimator [15] and the Cheng-Beaulieu estimators [16] are actually approximate solutions to the ML Nakagami m parameter estimation problem. This undesirable feature of the ML approach has, in part, motivated researchers to use a moment-based approach to find alternative Nakagami m parameter estimators.

2.2 Moment-Based m Parameter Estimation with Integer and Fractional Moments

In this section, we review some moment-based Nakagami m fading parameter estimators derived from analytical moment expressions of the Nakagami- m distribution.

2.2.1 Integer-Moment-Based m parameter Estimators

The k th moment expression for the Nakagami- m distribution is given by

$$\mu_k = \mathbb{E} \left[R^k \right] = \frac{\Gamma(m + k/2)}{\Gamma(m)} \left(\frac{\Omega}{m} \right)^{k/2}. \quad (2.3)$$

To avoid transcendental functions in deriving moment-based m parameter estimators, first we need to find a way to cancel the Gamma functions in (2.3).

Recall the iterative property of the Gamma function $\Gamma(z + 1) = z \cdot \Gamma(z)$, it is straightforward

to show that for even k values, $\Gamma(m + k/2)$ can be written as product of $\Gamma(m)$ and a polynomial function of m . Gamma functions in the moment expression can then be canceled, and a generally preferred algebraic equation is obtained. This is the basic idea of the moment-based Nakagami m parameter estimator proposed by Abdi and Kaveh [17]. For finite sample size, higher order sample moments may deviate from the value of the true moments significantly [18] (which is known as the outlier problem), smaller k values are preferred in this moment-based m parameter estimation scheme. However, the second order moment of the Nakagami- m distribution is simply the parameter Ω , which does not have parameter m in it. Therefore Abdi and Kaveh derived a moment-based m parameter estimator based on the fourth order moment expression of the Nakagami- m distribution. Substituting Ω in the fourth order moment expression by the second order sample moment, and then solve for m , a moment-based Nakagami m parameter estimator was found as [17]

$$\hat{m}_{INV} = \frac{\hat{\mu}_2^2}{\hat{\mu}_4 - \hat{\mu}_2^2} \quad (2.4)$$

where $\hat{\mu}_k = \frac{1}{N} \sum_{i=1}^N R_i^k$ is the k th order sample moment. This estimator was named the inverse normalized variance (INV) estimator, because it can be obtained by replacing the moments in the definition of m in (2.2) with the sample moments.

An alternative way to cancel the Gamma functions in (2.3) is to take the ratio of two different moments of the Nakagami- m distribution. Again by the iterative property of the Gamma function, we observe that the ratio of the k' th and k th moments, where $k' - k = a$ is a non-zero even integer, also formulates an algebraic equation which can be easily solved. The simplest case of this approach is to use $k' = 3$ and $k = 1$

$$\frac{\mu_3}{\mu_1} = \frac{\Gamma(m + 3/2)}{\Gamma(m + 1/2)} \left(\frac{\Omega}{m}\right) = \left(m + \frac{1}{2}\right) \left(\frac{\Omega}{m}\right). \quad (2.5)$$

Solving (2.5) for m with Ω substituted by its estimator, Cheng and Beaulieu derived another m

parameter estimator based on integer moments [19]

$$\hat{m}_t = \frac{\hat{\mu}_1 \hat{\mu}_2}{2(\hat{\mu}_3 - \hat{\mu}_1 \hat{\mu}_2)}. \quad (2.6)$$

Notice that the highest order of sample moments used in estimator \hat{m}_t is 3, which is smaller than that of \hat{m}_{INV} , therefore \hat{m}_t is expected to suffer from the outlier problem less than the INV estimator, which suggests a better estimation performance. This intuitive result will be confirmed by the asymptotic variance analysis in Section 2.2.3.

2.2.2 A Family of Fractional Moment-Based m Parameter Estimators

Cheng and Beaulieu observed that the INV estimator can also be derived by taking the ratio of the fourth and second moments of the Nakagami- m distribution and solving for parameter m [19]. This suggests that both estimators discussed in Section 2.2.1 belong to a family of moment-based Nakagami m parameter estimators derived by the ratio-of-moments approach. Notice that the order index k in the Nakagami- m moment expression (2.3) is not restricted to positive integers. This estimator family can thus be expanded into a family of fractional moment-based m parameter estimators. As briefly discussed in Section 2.2.1, because of the outlier problem, smaller moment order indices are preferred in this estimator family. Therefore admitting the use of fractional moments can actually result in better m parameter estimators. This novel idea was first introduced to Nakagami m parameter estimation by Cheng and Beaulieu in [19].

Based on the framework of the ratio-of-moments approach discussed in Section 2.2.1, and assuming that $k = 1/p$ and $k' = 2 + 1/p$, where p is a positive real number, the ratio of moments can then be expressed as

$$\frac{\mu_{2+1/p}}{\mu_{1/p}} = \frac{\Gamma(m + 1 + 1/2p)}{\Gamma(m + 1/2p)} \left(\frac{\Omega}{m}\right) = \left(m + \frac{1}{2p}\right) \left(\frac{\Omega}{m}\right). \quad (2.7)$$

Solving (2.7) and replacing the population moments with their sample counterparts, a general expression of this estimator family was found as [19]

$$\hat{m}_{1/p} = \frac{\hat{\mu}_{1/p} \hat{\mu}_2}{2p (\hat{\mu}_{2+1/p} - \hat{\mu}_{1/p} \hat{\mu}_2)}. \quad (2.8)$$

It is straightforward to show that when $p = 1$, $\hat{m}_{1/p}$ is actually \hat{m}_t , and \hat{m}_{INV} corresponds to a p value of 0.5.

However, when p approaches $+\infty$, (2.8) is found to have a $\frac{0}{0}$ indeterminate form after some algebraic manipulations. Therefore we need to go back to the population moment expression of (2.8) to find the expression for the limiting case.

Assuming $k = 1/p$ and recognizing that the limiting value of k is 0, we denote the limiting estimator as \hat{m}_0 . Then apply L'Hôpital's rule to the population moment expression of the estimator family, we have

$$\begin{aligned} \lim_{k \rightarrow 0} \frac{k \mu_k \mu_2}{2(\mu_{2+k} - \mu_k \mu_2)} &= \lim_{k \rightarrow 0} \frac{k \mathbb{E}[R^k] \mu_2}{2(\mathbb{E}[R^{2+k}] - \mathbb{E}[R^k] \mu_2)} \\ &= \lim_{k \rightarrow 0} \frac{\mu_2 (\mathbb{E}[R^k] + k \mathbb{E}[R^k \ln R])}{2 (\mathbb{E}[R^{2+k} \ln R] - \mu_2 \mathbb{E}[R^k \ln R])} \\ &= \frac{\mu_2}{2 (\mathbb{E}[R^2 \ln R] - \mu_2 \mathbb{E}[\ln R])} \\ &= \frac{\mu_2}{\mathbb{E}[R^2 \ln R^2] - \mu_2 \mathbb{E}[\ln R^2]}. \end{aligned} \quad (2.9)$$

Replacing the population moments and expected value expressions in (2.9) by their sample counterparts, the limiting estimator was found to be [20]

$$\hat{m}_0 = \frac{\hat{\mu}_2}{\frac{1}{N} \sum_{i=1}^N R_i^2 \ln R_i^2 - \hat{\mu}_2 \frac{1}{N} \sum_{i=1}^N \ln R_i^2}. \quad (2.10)$$

Combining (2.8) and (2.10) together and using the order index k consistently, we can rewrite

the fractional moment-based Nakagami m parameter estimator family as [19]

$$\hat{m}_k = \begin{cases} \frac{k\hat{\mu}_k\hat{\mu}_2}{2(\hat{\mu}_{2+k} - \hat{\mu}_k\hat{\mu}_2)}, & k > 0 \\ \frac{\hat{\mu}_2}{\frac{1}{N}\sum_{i=1}^N R_i^2 \ln R_i^2 - \hat{\mu}_2 \frac{1}{N}\sum_{i=1}^N \ln R_i^2}, & k = 0. \end{cases} \quad (2.11)$$

We observe for the estimator family (2.11), the smaller k is, the smaller the order sample moments that are used, and therefore better estimation performance is expected. In the limiting case, \hat{m}_0 should intuitively achieve the best performance among this fractional moment-based m parameter estimator family. Theoretical estimation performance analysis of this m parameter estimator family using the idea of asymptotic variance will be discussed in Section 2.2.3.

2.2.3 Large Sample Properties: Asymptotic Variance Analysis

For finite sample size, moment-based estimators are usually biased, do not have optimality properties, and their analytical performance are difficult to obtain. However, because of the consistency of moment-based estimators, we can derive their asymptotic variance analytically, which can be of great importance to performance analysis and comparison for large sample size scenarios.

The idea of asymptotic variance analysis of moment-based estimators is based on the central limit theorem and the weak law of large numbers (WLLN). The moment-based m parameter estimators discussed in this section are \sqrt{N} -consistent and asymptotically unbiased, thus the random variable $\sqrt{N}(\hat{m} - m)$, with \hat{m} a moment-based m parameter estimator, converges in law to a zero mean Gaussian random variable with variance σ^2

$$\sqrt{N}(\hat{m} - m) \xrightarrow{L} \mathcal{N}(0, \sigma^2) \quad \text{as } N \rightarrow +\infty. \quad (2.12)$$

The variance term σ^2 is the asymptotic variance of the corresponding moment-based m parameter estimator.

In the derivation of the asymptotic variance, we use an approach known as the multivariate delta method [21]. Take the moment-based estimator family with $k > 0$ as an example. For large sample size N , by the CLT, the vector $\sqrt{N}(\hat{\mu} - \mu)$ follows a trivariate Gaussian distribution $\mathcal{N}(\mathbf{0}, \Sigma_k)$. Here $\mu = (\mu_2, \mu_k, \mu_{k+2})$ is the population moment vector, $\hat{\mu} = (\hat{\mu}_2, \hat{\mu}_k, \hat{\mu}_{k+2})$ is the corresponding sample moment vector, and Σ_k is the covariance matrix of $\hat{\mu}$. Since the estimator \hat{m}_k in (2.11) is a function of the sample moments, the multivariate delta method says the asymptotic variance of \hat{m}_k can be derived from Σ_k using the *Jacobian* method [21].

The asymptotic variance σ_k^2 of the fractional moment-based m parameter estimator family (2.11) has been derived by Cheng [20] as

$$\sigma_k^2 = \begin{cases} m^2 \left[\frac{v_{2k}}{v_k^2} + \frac{v_{2k+2} - \frac{v_{k+2}^2}{v_2}}{(k/2)^2 v_k^2} \right], & k > 0 \\ m^2 [1 + m\psi'(m+1)], & k = 0 \end{cases} \quad (2.13)$$

where $v_k = \Gamma(m+k/2)/\Gamma(m)$, and $\psi(z) = d[\ln\Gamma(z)]/dz = \Gamma'(z)/\Gamma(z)$ is the digamma function.

2.3 Generalized Method of Moments Estimation

2.3.1 GMM Estimation for the Nakagami m Parameter

The basic idea used in the moment-based m parameter estimators reviewed in Section 2.2 is considered the classical method of moments, which aims to find a closed-form solution to a theoretical equation or equation set involving the moments of a distribution. The keystone of classical method of moments is to find a tractable equation set with moment conditions. However, desirable equations of moments like the algebraic equations derived in Section 2.2 for the Nakagami- m distribution are not always easy to find, even though closed-form analytical moment expressions are available.

The generalized method of moments estimation was first introduced by Hansen [10] in

econometrics literature and it is already a widely used method in this research area. However, to the author's best knowledge, this powerful method has not been applied to communications research. The GMM gives an alternative way to exploit moment conditions in estimation problems. It performs parameter estimation by minimizing weighted distances between population moments and their sample counterparts. Usually, more moment conditions than the number of unknown parameters are available in GMM estimation. The GMM provides a framework which combines all available moment conditions optimally for over-determined problems.

The most widely used implementation of the GMM method is an iterative regression process proposed by Hansen in his original GMM paper [10], namely Hansen's two-step GMM procedure. In this section, we follow Hansen's recipe to perform the Nakagami m parameter estimation with GMM.

With N *i.i.d.* realizations of a Nakagami- m random variable R_1, R_2, \dots, R_N and $s > 1$ population moment conditions $\mu_{k1}, \mu_{k2}, \dots, \mu_{ks}$, the GMM estimation for Nakagami m parameter is formulated as minimizing the orthogonal criterion function

$$Q(m; \mathbf{r}) = \mathbf{g}_N^T(m) \mathbf{W} \mathbf{g}_N(m) \quad (2.14)$$

where $\mathbf{r} = (R_1, R_2, \dots, R_N)^T$ is the observation vector, \mathbf{W} is a weighting matrix, and $\mathbf{g}_N(m)$ is the distance vector defined as

$$\mathbf{g}_N(m) = \begin{Bmatrix} \hat{\mu}_{k1} - \mu_{k1}(m) \\ \hat{\mu}_{k2} - \mu_{k2}(m) \\ \vdots \\ \hat{\mu}_{ks} - \mu_{ks}(m) \end{Bmatrix}. \quad (2.15)$$

In (2.15), $\hat{\mu}_{ki}$'s ($i = 1, 2, \dots, s$) are the (ki) th-order sample moments, and $\mu_{ki}(m)$'s denote the (ki) th-order population moment conditions as functions of the unknown parameter m . As discussed in Section 2.2, higher order sample moments may deviate from the population mo-

ments significantly, or we can say they are less accurate than lower order moment conditions. Therefore it is intuitively necessary to give higher order moment conditions less weight in the GMM framework. This is the purpose of introducing the weighting matrix \mathbf{W} . The accuracy of moment conditions can be measured by the variance covariance matrix of the sample moment statistics.

The first step of Hansen's recipe is to set $\mathbf{W} = \mathbf{I}$, the identity matrix. It means we first give the same weights to all moment conditions and solve for an initial estimate $\hat{m}^{(0)}$, which can be expressed as

$$\hat{m}^{(0)} = \underset{m}{\operatorname{argmin}} \mathbf{g}_N^T(m) \mathbf{g}_N(m). \quad (2.16)$$

The solution to the least squares (LS) problem in (2.16) can easily be found with software tools like MATLAB. Then we can use this initial estimate of the m parameter to obtain more precise estimates by an iterative regression process.

In the second step, we first compute the residue $\hat{\mathbf{u}}_t = \left[R_t^{k1} - \mu_{k1}(\hat{m}^{(0)}), R_t^{k2} - \mu_{k2}(\hat{m}^{(0)}), \dots, R_t^{ks} - \mu_{ks}(\hat{m}^{(0)}) \right]^T$ ($t = 1, 2, \dots, N$) for all N observations. Then the autocovariance matrices \mathbf{S}_j for lag length j is estimated by

$$\mathbf{S}_j = \frac{1}{N} \sum_{n=j+1}^N \hat{\mathbf{u}}_n \hat{\mathbf{u}}_{n-j}^T, \quad j = 0, 1, \dots, l \quad (2.17)$$

where l is the selected maximum lag length. With all l autocovariance matrices, we can estimate the long-run covariance matrix by

$$\hat{\mathbf{S}} = \hat{\mathbf{S}}_0 + \sum_{j=1}^l w_j (\hat{\mathbf{S}}_j + \hat{\mathbf{S}}_j^T) \quad (2.18)$$

where w_j 's are weights for autocovariance matrices with different lag values. Generally speaking, giving more distant lags less weight can improve estimation accuracy. A widely used weighting scheme is that of Bartlett [22], which is given by $w_j = 1 - j/(l+1)$. Then selecting

$\mathbf{W} = \hat{\mathbf{S}}^{-1}$, the second step estimate of the m parameter can be obtained as

$$\hat{m}^{(1)} = \underset{m}{\operatorname{argmin}} \mathbf{g}_N^T(m) \hat{\mathbf{S}}^{-1} \mathbf{g}_N(m). \quad (2.19)$$

Step 2 is then iterated until the absolute difference between two consecutive estimates is less than a predetermined threshold (estimation accuracy requirement) ε .

2.3.2 Derivation for Asymptotic Variance of the GMM Estimator

In Section 2.2.3 we have introduced the basic concept of asymptotic variance analysis and showed that the asymptotic variance of the fractional moment-based m parameter estimator family has been derived by Cheng [20]. However, for the GMM m parameter estimator, the asymptotic variance has not been derived in the engineering literature; besides, it is also unclear what is the best achievable performance among all possible m parameter estimators based on certain available moment conditions. Because the GMM provides a framework to optimally exploit all available moment conditions in its iteration process, it is natural to ask if the GMM attains the best asymptotic performance among all moment-based estimators using the same moment conditions. In this section, we derive the asymptotic variance of the GMM m parameter estimator introduced in Section 2.3.1.

Using the assumptions made in Section 2.3.1, we have N i.i.d. realizations of a Nakagami- m RV and $s > 1$ population moment conditions $\mu_{k1}, \mu_{k2}, \dots, \mu_{ks}$. For large sample size N , the joint distribution of the elements of $\mathbf{d} = (\hat{\mu}_{k1} - \mu_{k1}, \hat{\mu}_{k2} - \mu_{k2}, \dots, \hat{\mu}_{ks} - \mu_{ks})^T$ approaches a multi-variate Gaussian distribution $\mathcal{N}(\mathbf{0}, \Sigma)$, where Σ is the covariance matrix of elements of random vector \mathbf{d} , the difference vector between available population conditions and their sample counterparts. The element of Σ at the i th row and the j th column is $\Sigma_{ij} = \mu_{ki+kj} -$

2.3. Generalized Method of Moments Estimation

$\mu_{ki}\mu_{kj}$. Thus, the joint PDF of the observed sample moment vector $\hat{\mu} = (\hat{\mu}_{k1}, \hat{\mu}_{k2}, \dots, \hat{\mu}_{ks})^T$ is

$$f(\hat{\mu}_{k1}, \dots, \hat{\mu}_{ks}) = \frac{1}{(2\pi)^{\frac{s}{2}} [\mathbf{det}(\frac{\Sigma}{N})]^{\frac{1}{2}}} \exp \left[-(\hat{\mu}_{k1} - \mu_{k1}, \dots, \hat{\mu}_{ks} - \mu_{ks}) \left(\frac{\Sigma}{N}\right)^{-1} \begin{pmatrix} \hat{\mu}_{k1} - \mu_{k1} \\ \vdots \\ \hat{\mu}_{ks} - \mu_{ks} \end{pmatrix} \right] \quad (2.20)$$

where μ_i 's are functions of m and Ω , and $\mathbf{det}(\cdot)$ denotes the determinant of a square matrix.

The estimate \hat{m}_{GMM} in a maximum-likelihood sense can be expressed as

$$\begin{aligned} \hat{m}_{GMM} &= \operatorname{argmax}_m \ln f(\hat{\mu}_{k1}, \dots, \hat{\mu}_{ks}) \\ &= \operatorname{argmax}_m \left[-\frac{1}{2} \ln[\mathbf{det}(\Sigma)] - N(\hat{\mu}_{k1} - \mu_{k1}, \dots, \hat{\mu}_{ks} - \mu_{ks}) \Sigma^{-1} \begin{pmatrix} \hat{\mu}_{k1} - \mu_{k1} \\ \vdots \\ \hat{\mu}_{ks} - \mu_{ks} \end{pmatrix} + C \right] \end{aligned} \quad (2.21)$$

where C is a constant which does not depend on m .

For large sample size N , the quadratic term in (2.21) will be the dominant term. Thus, (2.21) can be well approximated by

$$\begin{aligned} \hat{m}_{GMM} &= \operatorname{argmin}_m (\hat{\mu}_{k1} - \mu_{k1}, \dots, \hat{\mu}_{ks} - \mu_{ks}) \Sigma^{-1} \begin{pmatrix} \hat{\mu}_{k1} - \mu_{k1} \\ \vdots \\ \hat{\mu}_{ks} - \mu_{ks} \end{pmatrix} \\ &= \operatorname{argmin}_m \mathbf{g}_N^T(m) \Sigma^{-1} \mathbf{g}_N(m) \\ &= \operatorname{argmin}_m Q(m; \hat{\mu}_{k1}, \dots, \hat{\mu}_{ks}) \end{aligned} \quad (2.22)$$

where $Q(m; \hat{\mu}_{k1}, \dots, \hat{\mu}_{ks})$ is the orthogonal criterion function (2.14). In the ML sense, the

estimate \hat{m}_{GMM} is the zero of the following function

$$\begin{aligned}
 & h(m; \hat{\mu}_{k1}, \dots, \hat{\mu}_{ks}) \\
 &= \frac{\partial Q(m; \hat{\mu}_{k1}, \dots, \hat{\mu}_{ks})}{\partial m} \\
 &= -2 \left(\frac{\partial \mu_{k1}}{\partial m}, \dots, \frac{\partial \mu_{ks}}{\partial m} \right) \Sigma^{-1} \begin{pmatrix} \hat{\mu}_{k1} - \mu_{k1} \\ \vdots \\ \hat{\mu}_{ks} - \mu_{ks} \end{pmatrix} \\
 &\quad - (\hat{\mu}_{k1} - \mu_{k1}, \dots, \hat{\mu}_{ks} - \mu_{ks}) \Sigma^{-1} \left(\frac{\partial \Sigma}{\partial m} \right) \Sigma^{-1} \begin{pmatrix} \hat{\mu}_{k1} - \mu_{k1} \\ \vdots \\ \hat{\mu}_{ks} - \mu_{ks} \end{pmatrix}
 \end{aligned} \tag{2.23}$$

in which we used the derivative identity of matrix inverse

$$\frac{\partial \Sigma^{-1}}{\partial m} = -\Sigma^{-1} \left(\frac{\partial \Sigma}{\partial m} \right) \Sigma^{-1}. \tag{2.24}$$

By the multivariate delta method [21], the asymptotic variance $\sigma_{GMM}^2 = \text{Var} [\sqrt{N} \hat{m}_{GMM}]$ can be obtained as

$$\sigma_{GMM}^2 = \left(\frac{\partial \hat{m}_{GMM}}{\partial \hat{\mu}_{k1}}, \dots, \frac{\partial \hat{m}_{GMM}}{\partial \hat{\mu}_{ks}} \right) \Sigma \begin{pmatrix} \frac{\partial \hat{m}_{GMM}}{\partial \hat{\mu}_{k1}} \\ \vdots \\ \frac{\partial \hat{m}_{GMM}}{\partial \hat{\mu}_{ks}} \end{pmatrix} \bigg|_{\hat{\mu}_{k1}=\mu_{k1}, \dots, \hat{\mu}_{ks}=\mu_{ks}}. \tag{2.25}$$

Consider $h(\hat{m}_{GMM}; \hat{\mu}_{k1}, \dots, \hat{\mu}_{ks}) = 0$ as an implicit function of \hat{m}_{GMM} in terms of $(\hat{\mu}_{k1}, \dots, \hat{\mu}_{ks})$.

We write the derivative of the implicit function as

$$\begin{cases} \frac{\partial h(\hat{m}_{GMM}; \hat{\mu}_{k1}, \dots, \hat{\mu}_{ks})}{\partial \hat{m}_{GMM}} \frac{\partial \hat{m}_{GMM}}{\partial \hat{\mu}_{k1}} + \frac{\partial h(\hat{m}_{GMM}; \hat{\mu}_{k1}, \dots, \hat{\mu}_{ks})}{\partial \hat{\mu}_{k1}} = 0 \\ \vdots \\ \frac{\partial h(\hat{m}_{GMM}; \hat{\mu}_{k1}, \dots, \hat{\mu}_{ks})}{\partial \hat{m}_{GMM}} \frac{\partial \hat{m}_{GMM}}{\partial \hat{\mu}_{ks}} + \frac{\partial h(\hat{m}_{GMM}; \hat{\mu}_{k1}, \dots, \hat{\mu}_{ks})}{\partial \hat{\mu}_{ks}} = 0 \end{cases} \quad (2.26)$$

and have

$$\begin{pmatrix} \frac{\partial \hat{m}_{GMM}}{\partial \hat{\mu}_{k1}} \\ \vdots \\ \frac{\partial \hat{m}_{GMM}}{\partial \hat{\mu}_{ks}} \end{pmatrix} = - \frac{1}{\frac{\partial h(\hat{m}_{GMM}; \hat{\mu}_{k1}, \dots, \hat{\mu}_{ks})}{\partial \hat{m}_{GMM}}} \begin{pmatrix} \frac{\partial h(\hat{m}_{GMM}; \hat{\mu}_{k1}, \dots, \hat{\mu}_{ks})}{\partial \hat{\mu}_{k1}} \\ \vdots \\ \frac{\partial h(\hat{m}_{GMM}; \hat{\mu}_{k1}, \dots, \hat{\mu}_{ks})}{\partial \hat{\mu}_{ks}} \end{pmatrix}. \quad (2.27)$$

Calculating the partial derivatives of $h(\hat{m}_{GMM}; \hat{\mu}_{k1}, \dots, \hat{\mu}_{ks})$ in (2.27) and substitute (2.27) into (2.25), the asymptotic variance of the GMM m parameter estimator can be written as

$$\sigma_{GMM}^2 = \frac{1}{\eta} \quad (2.28)$$

where η is defined as

$$\eta = \left(\frac{\partial \mu_{k1}}{\partial m} \Big|_{m=\hat{m}_{GMM}}, \dots, \frac{\partial \mu_{ks}}{\partial m} \Big|_{m=\hat{m}_{GMM}} \right) \Sigma^{-1} \begin{pmatrix} \frac{\partial \mu_{k1}}{\partial m} \Big|_{m=\hat{m}_{GMM}} \\ \vdots \\ \frac{\partial \mu_{ks}}{\partial m} \Big|_{m=\hat{m}_{GMM}} \end{pmatrix}. \quad (2.29)$$

A detailed derivation of (2.28) is given in Appendix A. Because of the consistency of the GMM estimation scheme, for large sample size N , the asymptotic variance of \hat{m}_{GMM} can be further simplified as

$$\sigma_{GMM}^2 = \left[\left(\frac{\partial \mu_{k1}}{\partial m}, \dots, \frac{\partial \mu_{ks}}{\partial m} \right) \Sigma^{-1} \begin{pmatrix} \frac{\partial \mu_{k1}}{\partial m} \\ \vdots \\ \frac{\partial \mu_{ks}}{\partial m} \end{pmatrix} \right]^{-1}. \quad (2.30)$$

2.4 Numerical Results and Discussion

In this section, we present performance comparisons of several moment-based m parameter estimators. Both mean square error (MSE) analysis via Monte Carlo simulation and the asymptotic variance analysis are conducted for the classical moment-based estimators reviewed in Section 2.2 and the GMM estimator introduced in Section 2.3.

Since estimators discussed in this chapter are considered asymptotically unbiased, we use performance of the ML approach as a benchmark in the comparison. The MSE performance of the moment-based estimators are compared with the Cramér-Rao lower bound. For asymptotic variance analysis, we compute the asymptotic relative efficiency (ARE) [21] of different moment-based m parameter estimators with respect to the ML-based estimator. The relative efficiency $e_{Z_1 Z_0}$ of estimator \hat{Z}_1 to \hat{Z}_0 is defined as

$$e_{Z_1 Z_0} = \frac{\text{Var}(\hat{Z}_0)}{\text{Var}(\hat{Z}_1)}. \quad (2.31)$$

The ARE of the ML-based estimator with respect to itself is thus 1. The ARE of the moment-based estimators with respect to ML should be less than 1 because moment statistics are not the sufficient statistics.

Fig. 2.1 and Fig. 2.2 show the simulated MSE performance and the asymptotic relative efficiency of the moment-based Nakagami m parameter estimators respectively. We observe that for all values of m , the limiting estimator of the fractional moment-based estimator family (2.11) and the GMM estimator with first, second and third order moment conditions are more efficient than the other moment-based m parameter estimators. Specifically, when $m < 1$, the limiting fractional moment-based estimator achieves the best estimation performance; whereas when $m > 1$, the GMM estimator based on the first three integer moments outperforms the limiting estimator. The performance difference between the GMM estimator based on the first two integer moments and the GMM estimator based on the first three integer moments

suggests that the GMM approach can achieve better estimation performance by adding more moment conditions. It is interesting to notice that the INV estimator which uses the second and fourth order moments achieves the same MSE and asymptotic variance as the GMM estimator based on the same moment conditions. This implies that the INV estimator has achieved the best asymptotic performance among all MoM estimators based on the second and fourth order moment conditions. However, we can observe that there is a huge performance gap between the GMM estimator with the first three integer moment conditions and the classical moment-based estimator \hat{m}_t . This observation suggests that based on the same moment conditions, it is still possible to design a moment-based estimator with better performance than that of \hat{m}_t .

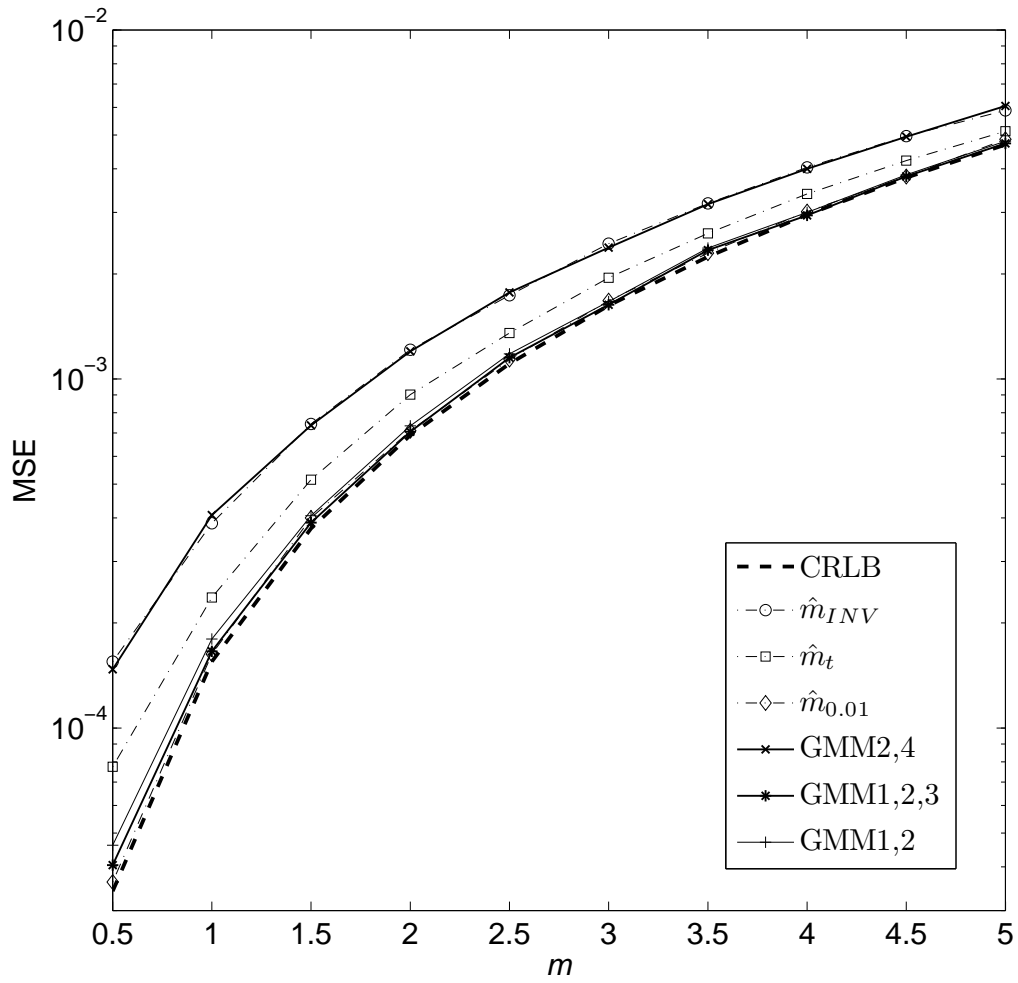


Figure 2.1: Simulated MSE performance of moment-based Nakagami fading parameter estimators with sample size $N = 10,000$.

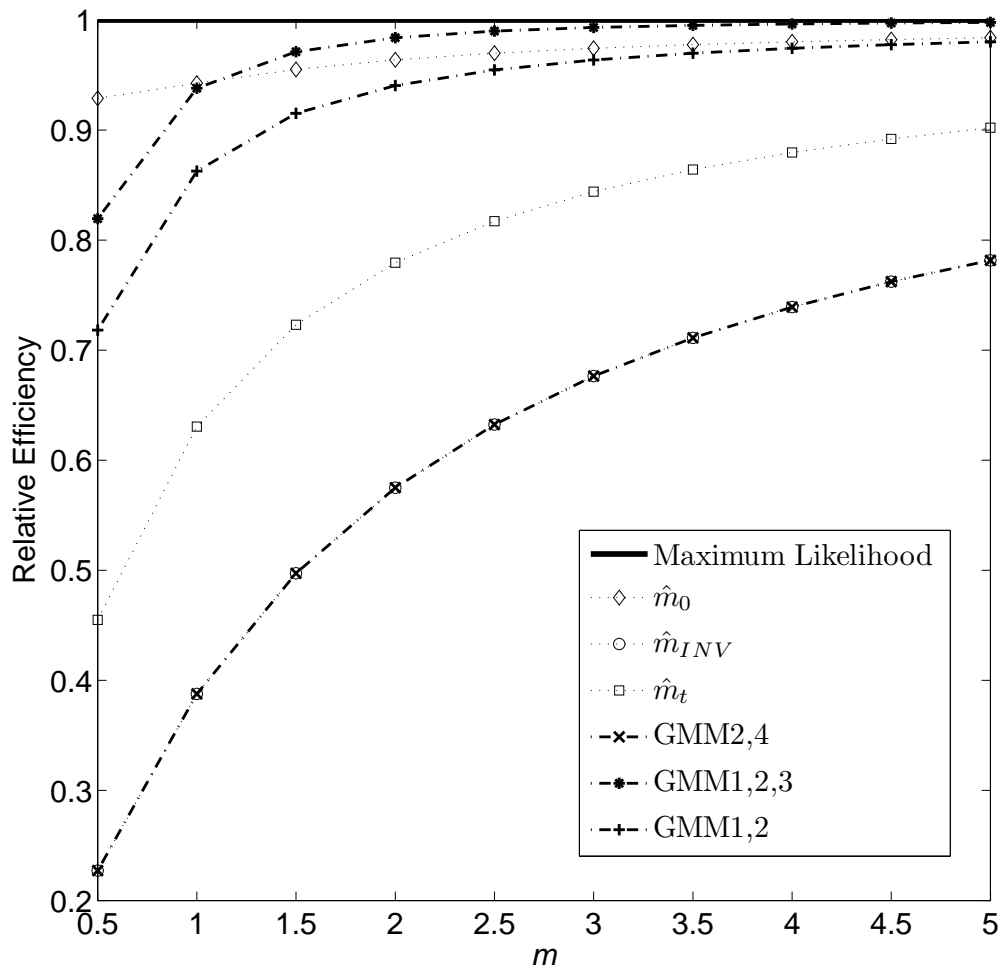


Figure 2.2: Asymptotic relative estimation efficiencies of moment-based Nakagami fading parameter estimators with respect to ML.

2.5 Summary

In this chapter, we have provided a detailed discussion on moment-based estimation for the Nakagami- m fading model. A family of classical moment-based m parameter estimators based on both integer and fractional moments has been reviewed. It has been shown that some commonly used moment-based m parameter estimators are special cases of this estimator family. The GMM estimation approach which exploits all available moment conditions in a determined or over-determined estimation problem has been introduced to fading parameter estimation for the first time. Systematic performance comparison for moment-based m parameter estimators has been conducted by both Monte Carlo simulation and asymptotic variance analysis.

Chapter 3

On Statistics of Logarithmic Ratio of Arithmetic Mean to Geometric Mean for Nakagami- m Fading Power

Chapter 2 discusses several moment-based Nakagami m parameter estimators. In this chapter, we focus on performance analysis of maximum-likelihood based m parameter estimators.

3.1 ML-Based Nakagami- m Parameter Estimators

Recall that the PDF of the Nakagami- m fading envelope R is given by

$$f_R(r) = \frac{2}{\Gamma(m)} \left(\frac{m}{\Omega}\right)^m r^{2m-1} \exp\left(-\frac{m}{\Omega}r^2\right), \quad r \geq 0, \quad m \geq \frac{1}{2} \quad (3.1)$$

where $\Omega = \mathbb{E}[R^2]$ is the scale parameter, and the shape parameter m is defined as

$$m = \frac{\Omega^2}{\mathbb{E}[(R^2 - \Omega)^2]}, \quad m \geq \frac{1}{2}. \quad (3.2)$$

As briefly discussed in Chapter 1, in order to characterize wireless channels using the Nakagami- m distribution, it is crucial to determine or estimate the value of m from N random samples R_1, R_2, \dots, R_N drawn independently according to (3.1). Several methods for estimating the m parameter have been reported in literature. The Greenwood-Durand estimator (GDE)

[15], a ML-based Gamma-shape parameter estimator, is given by

$$\hat{m}_{GDE} = \begin{cases} f_1(\Delta) & \Delta < 0.5772 \\ f_2(\Delta) & 0.5772 \leq \Delta \leq 17 \end{cases} \quad (3.3)$$

where

$$f_1(\Delta) = \frac{0.5000876 + 0.1648852\Delta - 0.0544274\Delta^2}{\Delta} \quad (3.4a)$$

$$f_2(\Delta) = \frac{8.898919 + 9.059950\Delta - 0.9775373\Delta^2}{(17.79728 + 11.968477\Delta + \Delta^2)\Delta} \quad (3.4b)$$

and

$$\Delta = \ln \left[\frac{1}{N} \sum_{i=1}^N R_i^2 \right] - \frac{1}{N} \sum_{i=1}^N \ln R_i^2 = -\psi(\hat{m}) + \ln(\hat{m}) \quad (3.5)$$

in which $\psi(\cdot)$ is the digamma function defined as $\psi(x) = \Gamma'(x)/\Gamma(x)$. More recently, Cheng and Beaulieu [16] proposed to use the first-order and second-order approximations to $\psi(\cdot)$ in ML-based m parameter estimation and derived two approximate ML estimators for m as

$$\hat{m}_1 = \frac{1}{2\Delta} \quad (3.6)$$

and

$$\hat{m}_2 = \frac{6 + \sqrt{36 + 48\Delta}}{24\Delta}. \quad (3.7)$$

It was pointed out by Zhang [23] that estimators similar to (3.6) and (3.7) were reported earlier by Thom [24] in the estimation problem for the Gamma distribution in another discipline.

The ML-based estimators presented in (3.3), (3.6), and (3.7) are all functions of the parameter Δ . This immediately implies that if we know the PDF of the parameter Δ , we can assess the performance of ML-based estimators for the Nakagami m parameter without performing intensive computer simulations.

3.2 Statistical Properties of Δ

3.2.1 Alternative Expression of Δ

The expression of parameter Δ in (3.5) can be written as

$$\Delta = \ln \left(\frac{1}{N} \sum_{i=1}^N R_i^2 \right) - \ln \left[\left(\prod_{i=1}^N R_i^2 \right)^{\frac{1}{N}} \right] = \ln \left[\frac{\frac{1}{N} \sum_{i=1}^N R_i^2}{\left(\prod_{i=1}^N R_i^2 \right)^{\frac{1}{N}}} \right]. \quad (3.8)$$

We observe from (3.8) that the parameter Δ is just the logarithmic ratio of the arithmetic mean to the geometric mean of N samples of the Nakagami- m fading power.

It can also be shown that the Nakagami- m distribution is a member of a two-parameter exponential family, and the parameter Δ is a function of the joint complete sufficient statistics. The detailed proof is given in Appendix B. In addition, by properties of sufficient statistics [25], the ML-based estimator of the unknown parameter is a function of the sufficient statistic.

3.2.2 Nonnegative Property of Δ

According to the well-known Arithmetic-Geometric inequality [26], we have

$$\frac{1}{N} \sum_{i=1}^N R_i^2 \geq \left(\prod_{i=1}^N R_i^2 \right)^{\frac{1}{N}} \quad (3.9)$$

and therefore we must have $\Delta > 0$. By recognizing the fact that when m approaches $+\infty$ the Nakagami PDF becomes an impulse function located at $\sqrt{\Omega}$, we arrive at

$$\lim_{m \rightarrow +\infty} \Delta = \lim_{m \rightarrow +\infty} \ln \left[\frac{\frac{1}{N} \sum_{i=1}^N R_i^2}{\left(\prod_{i=1}^N R_i^2 \right)^{\frac{1}{N}}} \right] = \ln \left[\frac{\frac{1}{N} \sum_{i=1}^N \Omega}{\left(\prod_{i=1}^N \Omega \right)^{\frac{1}{N}}} \right] = 0. \quad (3.10)$$

3.2.3 Moment Generating Function of Δ

To derive the MGF of Δ , denoted by $\Phi_{\Delta}(s)$, we start with the definition and have

$$\begin{aligned}
 \Phi_{\Delta}(s) &= \mathbb{E} \left[e^{s\Delta} \right] \\
 &= \underbrace{\int_0^{+\infty} \cdots \int_0^{+\infty}}_N \left[\frac{(\sum_{i=1}^N R_i^2)^s}{N^s (\prod_{i=1}^N R_i^2)^{\frac{s}{N}}} \right] \\
 &\quad \times \left[\frac{2}{\Gamma(m)} \left(\frac{m}{\Omega} \right)^m R_1^{2m-1} e^{-\frac{m}{\Omega} R_1^2} \right] \times \cdots \times \left[\frac{2}{\Gamma(m)} \left(\frac{m}{\Omega} \right)^m R_N^{2m-1} e^{-\frac{m}{\Omega} R_N^2} \right] dR_1 \cdots dR_N \\
 &= \frac{\left[\frac{2}{\Gamma(m)} \left(\frac{m}{\Omega} \right)^m \right]^N}{N^s} \underbrace{\int_0^{+\infty} \cdots \int_0^{+\infty}}_N \prod_{i=1}^N R_i^{2m-\frac{2s}{N}-1} \cdot \left(\sum_{i=1}^N R_i^2 \right)^s \exp \left(-\frac{m}{\Omega} \sum_{i=1}^N R_i^2 \right) dR_1 \cdots dR_N.
 \end{aligned} \tag{3.11}$$

If we let $d = m - s/N$, after a change of variable ($R_i^2 = x_i$), we obtain

$$\Phi_{\Delta}(s) = \frac{\left[\frac{1}{\Gamma(m)} \left(\frac{m}{\Omega} \right)^m \right]^N}{N^s} \underbrace{\int_0^{+\infty} \cdots \int_0^{+\infty}}_N \prod_{i=1}^N x_i^{d-1} \cdot \left(\sum_{i=1}^N x_i \right)^s \cdot \exp \left(-\frac{m}{\Omega} \sum_{i=1}^N x_i \right) dx_1 \cdots dx_N. \tag{3.12}$$

The multiple N integrals in (3.12) can be reduced to a single integral by invoking the following useful integral identity [27]

$$\begin{aligned}
 &\underbrace{\int_0^{+\infty} \cdots \int_0^{+\infty}}_n x_1^{\alpha_1-1} x_2^{\alpha_2-1} \cdots x_n^{\alpha_n-1} f\left(\sum_{i=1}^n x_i\right) dx_1 \cdots dx_n \\
 &= \frac{\Gamma(\alpha_1)\Gamma(\alpha_2)\cdots\Gamma(\alpha_n)}{\Gamma(\alpha_1 + \alpha_2 + \cdots + \alpha_n)} \int_0^{+\infty} u^{\alpha_1+\alpha_2+\cdots+\alpha_n-1} f(u) du.
 \end{aligned} \tag{3.13}$$

Letting $\alpha_1 = \alpha_2 = \dots = \alpha_N = d$ and $f(x) = x^s \exp(-\frac{m}{\Omega}x)$, we obtain a compact form for the MGF of Δ as

$$\begin{aligned}\Phi_{\Delta}(s) &= \frac{\left[\frac{1}{\Gamma(m)} \left(\frac{m}{\Omega}\right)^m\right]^N}{N^s} \cdot \frac{[\Gamma(d)]^N}{\Gamma(Nd)} \cdot \int_0^{+\infty} u^{Nd-1} u^s \exp\left(-\frac{m}{\Omega}u\right) du \\ &= \frac{\Gamma(mN)[\Gamma(m-s/N)]^N}{N^s [\Gamma(m)]^N \Gamma(mN-s)}\end{aligned}\quad (3.14)$$

where in obtaining the last step we have used the definition of the Gamma function.

3.2.4 Probability Density Function of Δ

The PDF of Δ can be obtained from its MGF by applying an inverse Laplace transform as

$$\begin{aligned}f_{\Delta}(\delta) &= \frac{1}{2\pi j} \int_{c-j\infty}^{c+j\infty} \Phi_{\Delta}(-s) e^{s\delta} ds \\ &= \frac{\Gamma(mN)}{[\Gamma(m)]^N} \cdot \frac{1}{2\pi j} \int_{c-j\infty}^{c+j\infty} \frac{N^s [\Gamma(m+s/N)]^N}{\Gamma(mN+s)} e^{s\delta} ds\end{aligned}\quad (3.15)$$

where $j^2 = -1$ and c is a suitably chosen positive constant which ensures that the contour path is in the region of convergence. The integration is taken along the vertical line $\Re\{s\} = c$ in the complex plane such that c is greater than the real part of any singularity of $\Phi_{\Delta}(-s)$.

If we now let $y = s/N$, the PDF becomes

$$f_{\Delta}(\delta) = \frac{\Gamma(mN)}{[\Gamma(m)]^N} \cdot \frac{N}{2\pi j} \int_{c'-j\infty}^{c'+j\infty} \frac{N^{Ny} [\Gamma(m+y)]^N}{\Gamma[N(m+y)]} e^{Ny\delta} dy \quad (3.16)$$

where $c' = c/N$ is another positive constant. With the aid of the Gauss multiplication theorem [28]

$$\Gamma(nx) = (2\pi)^{\frac{1-n}{2}} n^{nx-\frac{1}{2}} \prod_{k=0}^{n-1} \Gamma\left(x + \frac{k}{n}\right) \quad (3.17)$$

we arrive at

$$\begin{aligned}
 f_{\Delta}(\delta) &= \frac{N \cdot \Gamma(mN)}{[\Gamma(m)]^N} \cdot \frac{1}{2\pi j} \cdot \int_{c'-j\infty}^{c'+\infty} \frac{N^{Ny} [\Gamma(m+y)]^N}{(2\pi)^{\frac{1-N}{2}} N^{N(m+y)-\frac{1}{2}} \prod_{k=1}^{N-1} \Gamma\left[m+y+\frac{k}{N}\right]} (e^{N\delta})^y dy \\
 &= N \cdot \frac{\Gamma(mN)}{(2\pi)^{\frac{1-N}{2}} N^{Nm-\frac{1}{2}} [\Gamma(m)]^N} \cdot \frac{1}{2\pi j} \cdot \int_{c'-j\infty}^{c'+j\infty} \frac{\prod_{k=1}^N \Gamma\left[1-(1-m)+y\right]}{\prod_{k=0}^{N-1} \Gamma\left[1-(1-m-\frac{k}{N})+y\right]} (e^{N\delta})^y dy
 \end{aligned} \tag{3.18}$$

Now applying the definition of Meijer's G -function [29]

$$G_{p,q}^{m,n} \left(z \left| \begin{array}{c} a_1 \quad \cdots \quad a_p \\ b_1 \quad \cdots \quad b_q \end{array} \right. \right) = \frac{1}{2\pi j} \int \frac{\prod_{j=1}^m \Gamma(b_j - s) \prod_{j=1}^n \Gamma(1 - a_j + s)}{\prod_{j=m+1}^q \Gamma(1 - b_j + s) \prod_{j=n+1}^p \Gamma(a_j - s)} \cdot z^s ds \tag{3.19}$$

to (3.18), we can simply write the PDF of Δ as

$$f_{\Delta}(\delta) = N\xi \cdot G_{N,N}^{0,N} \left(e^{N\delta} \left| \begin{array}{c} 1-m \quad \cdots \quad 1-m \\ 1-m \quad \cdots \quad 1-m - \frac{N-1}{N} \end{array} \right. \right) \tag{3.20}$$

where

$$\xi = \frac{\Gamma(mN)}{(2\pi)^{\frac{1-N}{2}} N^{Nm-\frac{1}{2}} [\Gamma(m)]^N} \tag{3.21}$$

Computer simulations were carried out to generate empirical PDFs of Δ for different m and N values, and to compare them with the analytical PDFs obtained from (3.20). Fig. 3.1 shows the analytical and empirical PDFs of Δ for $m = 0.5, 1, 2$ when $N = 5$. Fig. 3.2 shows the analytical and empirical PDFs of Δ for $m = 0.5, 1, 2$ when $N = 10$. It is shown that the analytical PDFs of Δ have excellent agreement with the empirical ones.

When the sample size N becomes large, the latest version of commercial software such as MAPLE and MATHEMATICA are incapable of evaluating our analytical PDF expression in (3.20).

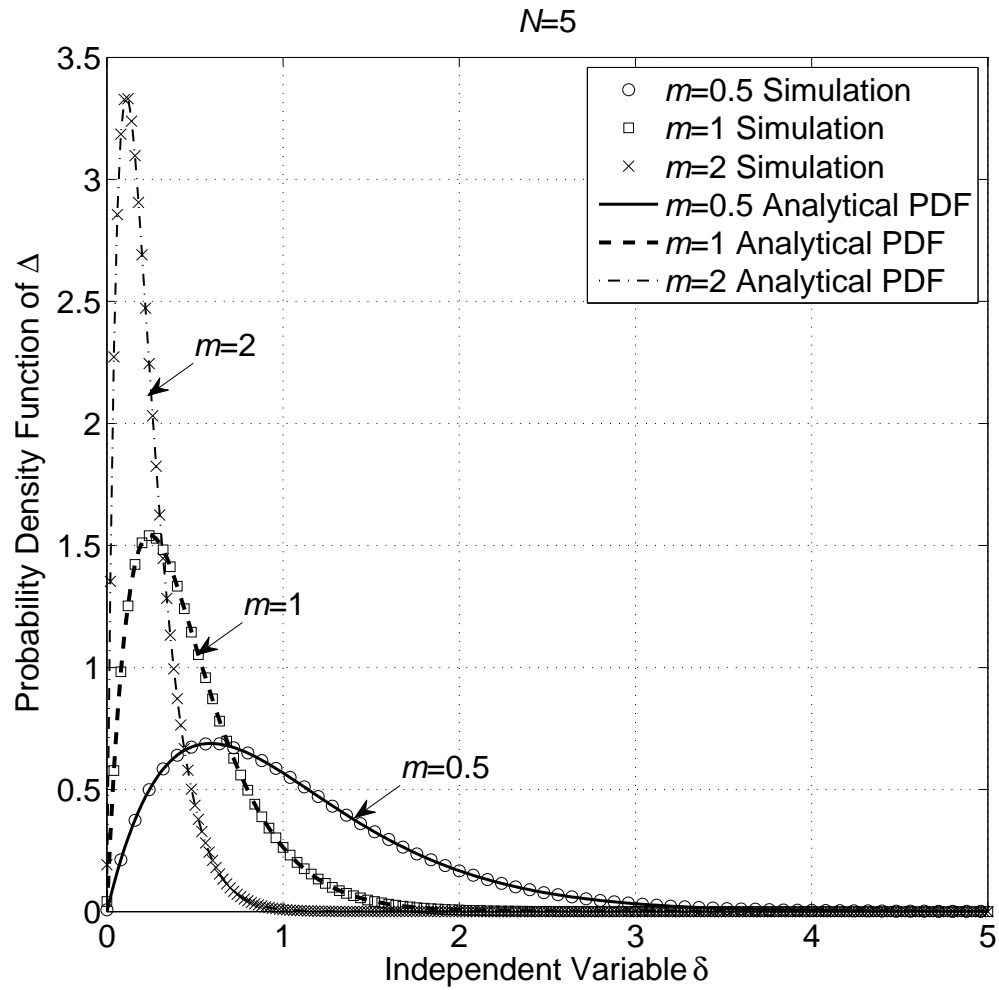


Figure 3.1: Comparison of empirical PDFs and analytical PDFs of Δ for $m = 0.5, 1, 2$ with sample size $N = 5$.

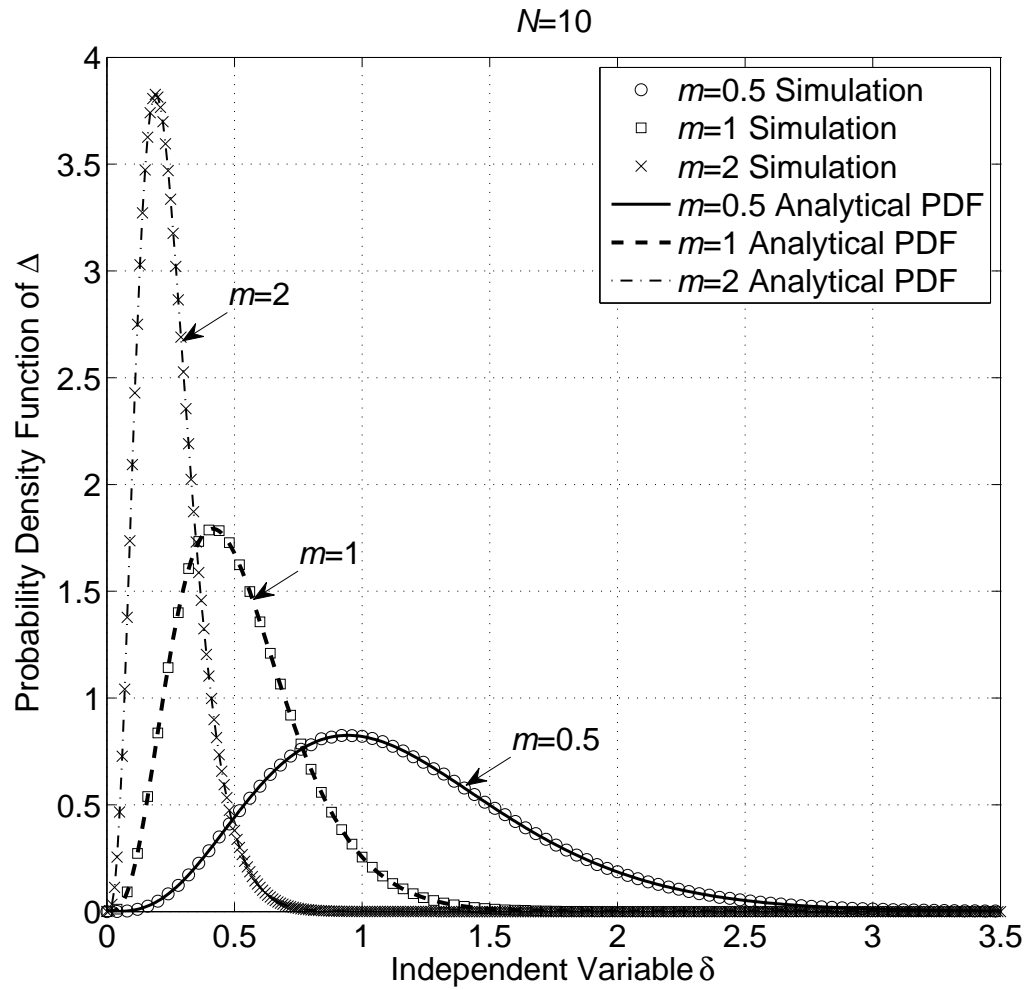


Figure 3.2: Comparison of empirical PDFs and analytical PDFs of Δ for $m = 0.5, 1, 2$ with sample size $N = 10$.

3.3 Gamma Approximation

To avoid the high computational complexity associated with the Meijer's G -function for large N , we are motivated to approximate the PDF of Δ using another PDF which can be easily evaluated and is analytically tractable.

3.3.1 Gamma Approximation for PDF of Δ

From the nonnegative property discussed in Section 3.2, we know that Δ is defined on $[0, +\infty)$. We propose to use a two-parameter Gamma PDF, which is also defined on $[0, +\infty)$, to approximate the PDF of Δ . To determine the parameters θ and k in the two-parameter Gamma PDF

$$f_X(x) = \frac{x^{k-1} e^{-x/\theta}}{\theta^k \Gamma(k)}, \quad x \geq 0; \theta, k > 0 \quad (3.22)$$

we can simply match the mean and variance of the two-parameter Gamma distribution to the mean and variance of Δ .

From the MGF of Δ in (3.14), the first two moments of Δ can be obtained by taking the first and the second derivatives of the MGF with respect to s and evaluating the results at $s = 0$. It is straightforward to show that the first two moments of Δ are given by

$$\mu_1 = -\psi(m) - \ln(N) + \psi(mN) \quad (3.23a)$$

$$\begin{aligned} \mu_2 = & [\psi(m)]^2 + [\ln(N)]^2 + [\psi(mN)]^2 + 2\psi(m) \ln(N) \\ & - 2\psi(m)\psi(mN) - 2\psi(mN) \ln(N) + \frac{1}{N} \psi'(m) - \psi'(mN). \end{aligned} \quad (3.23b)$$

Setting the mean and variance of the two-parameter Gamma distribution equal to the mean and

variance of Δ

$$\mu_1 = k\theta \quad (3.24a)$$

$$\mu_2 - (\mu_1)^2 = k\theta^2 \quad (3.24b)$$

we arrive at

$$\theta = \frac{\frac{1}{N}\psi'(m) - \psi'(mN)}{-\psi(m) - \ln(N) + \psi(mN)} \quad (3.25a)$$

$$k = \frac{\frac{1}{N}\psi'(m) - \psi'(mN)}{[-\psi(m) - \ln(N) + \psi(mN)]^2}. \quad (3.25b)$$

The two-parameter Gamma approximation is desirable since this PDF has a simple exponential form, which can be easily evaluated and manipulated in practice.

3.3.2 Validating the Gamma Approximation

Computer simulations were also carried out to compare the two-parameter Gamma approximate PDFs with the empirical PDFs of Δ .

Fig. 3.3 shows the comparison between the empirical PDFs and the Gamma approximated PDFs of Δ for $m = 0.5, 1, \text{ and } 2$ with $N = 10$. Fig. 3.4 presents the comparison between the empirical PDFs and the corresponding Gamma PDFs for $m = 0.5, 1, \text{ and } 2$ with $N = 100$. Both Figs. 3.3 and 3.4 demonstrate that the two-parameter Gamma PDF is a good candidate for approximating the PDF of Δ .

To numerically validate the feasibility of approximating Δ as a Gamma RV, we use the Kolmogorov-Smirnov (K-S) test for goodness-of-fit. The basic idea of the K-S test is to compare the empirical cumulative distribution function (CDF) with the CDF of the hypothesized distribution. The test statistic D_n for test sample volume n is defined as the supremum of the

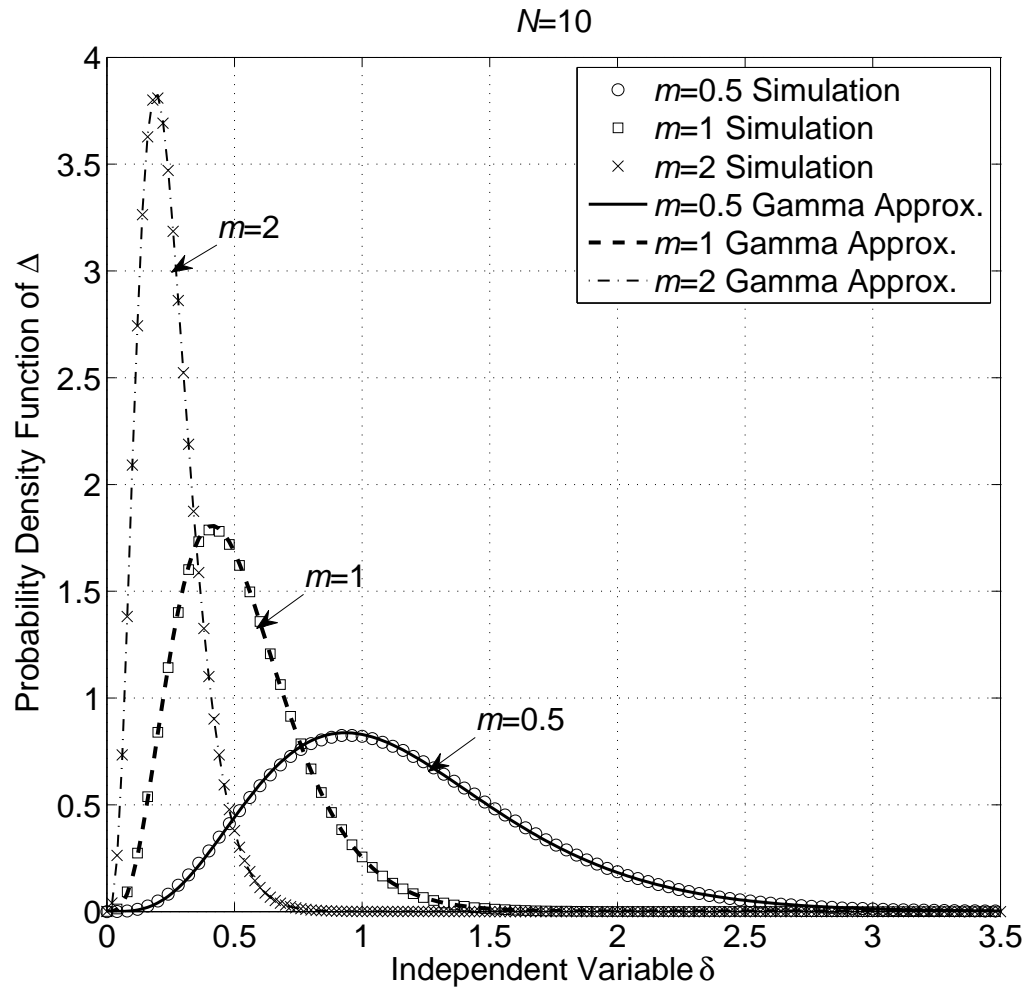


Figure 3.3: Comparison of empirical PDFs and Gamma approximated PDFs of Δ for $m = 0.5, 1, 2$ with sample size $N = 10$.

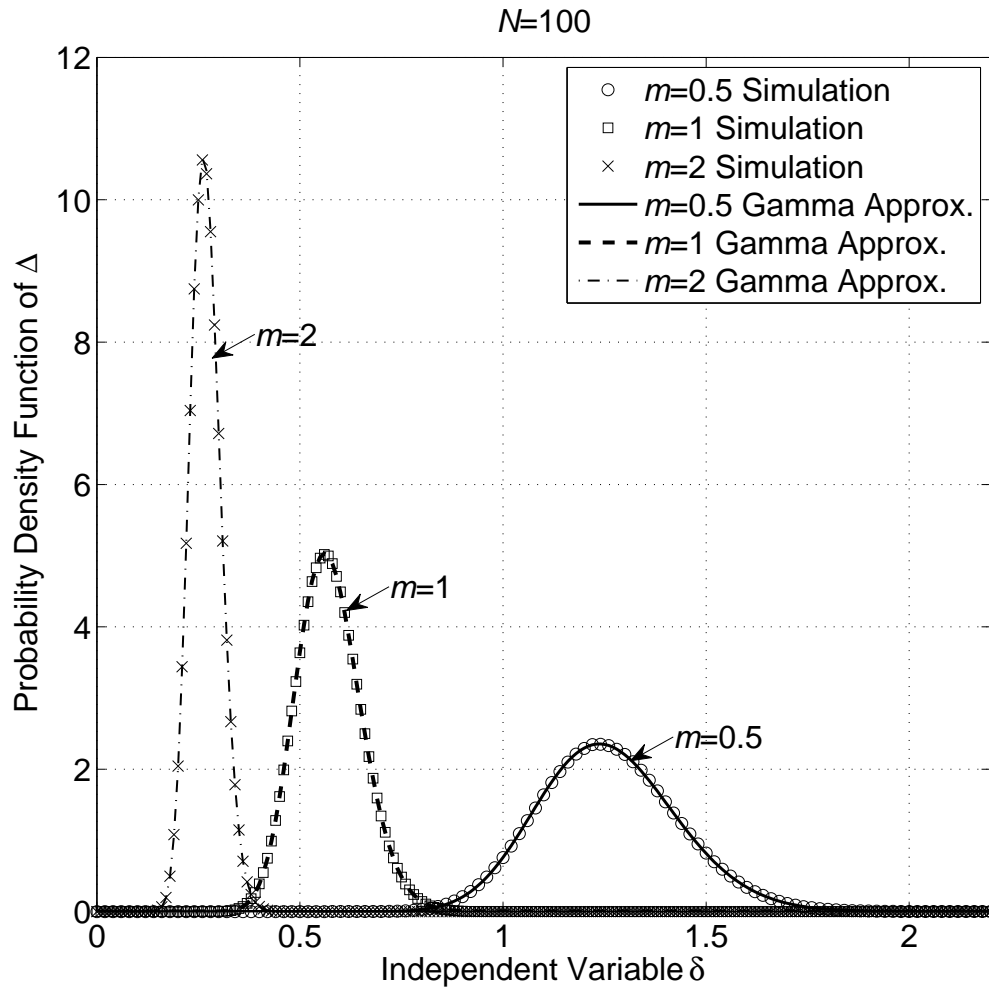


Figure 3.4: Comparison of empirical PDFs and Gamma approximated PDFs of Δ for $m = 0.5, 1, 2$ with sample size $N = 100$.

3.3. Gamma Approximation

Table 3.1: Kolmogorov-Smirnov test for goodness-of-fit for the Gamma approximation.

	$n = 100$			$n = 1,000$		
	D_{max}	D_{avg}	$Acpt. \%$	D_{max}	D_{avg}	$Acpt. \%$
$N = 10$						
$m = 0.5$	0.226	0.085	99.03%	0.067	0.027	99.05%
$m = 1$	0.218	0.085	98.87%	0.069	0.027	98.83%
$m = 2$	0.226	0.085	99.01%	0.072	0.027	99.00%
$m = 5$	0.232	0.085	99.11%	0.078	0.027	99.01%
$N = 100$						
$m = 0.5$	0.212	0.085	98.95%	0.075	0.027	99.00%
$m = 1$	0.222	0.085	99.11%	0.066	0.027	98.91%
$m = 2$	0.211	0.085	99.00%	0.074	0.027	99.03%
$m = 5$	0.232	0.085	99.01%	0.068	0.027	98.88%

absolute difference between the theoretical CDF $F(x)$ and the empirical CDF $F_n(x)$

$$D_n \equiv \sup_{x \in [0, +\infty)} |F(x) - F_n(x)|. \quad (3.26)$$

If the test statistic D_n is less than a critical value D_n^α , which is determined by both the test sample volume n (degree of freedom) and a prescribed significance level α , the theoretical distribution is acceptable at a confidence level of $1 - \alpha$.

Case studies were conducted using test sample volume $n = 100$ and $1,000$ for $m = 0.5, 1, 2$, and 5 with $N = 10$ and 100 . The significance level α was chosen to be 0.01 , giving a 99.00% confidence level for the K-S test.

Table 3.1 shows the maximum test statistics D_{max} and the average test statistics D_{avg} obtained from $10,000$ experiments conducted in our study. According to [30], the critical values for test sample volume $n = 100$ and $1,000$ at significance level 0.01 are $D_{100}^{0.01} = 1.63/\sqrt{100} = 0.163$ and $D_{1,000}^{0.01} = 1.63/\sqrt{1000} = 0.0515$ respectively. We observe that in each case of our case studies, about 99% of the experiments accepted the hypothesis that the random variable Δ can be modelled as a Gamma random variable at a confidence level of 99.00% . Table 3.1 also shows that D_{max} values, under which the hypothesis is rejected, are slightly greater than

Table 3.2: Numerical MSE performance evaluations for ML-based Nakagami m parameter estimators.

$N = 100$			
	$\mathbb{E}[\cdot]$	$\text{Var}[\cdot]$	Bias
\hat{m}_1			
$m = 0.5$	0.40413731	0.00311112	-0.09586269
$m = 1$	0.89122741	0.01615511	-0.10877259
$m = 2$	1.90478583	0.07568833	-0.09521418
$m = 5$	4.98725469	0.52291930	-0.01274531
\hat{m}_2			
$m = 0.5$	0.530691584	0.00348994	0.03069158
$m = 1$	1.034506216	0.01677922	0.03450622
$m = 2$	2.058782448	0.07652349	0.05878245
$m = 5$	5.148600611	0.52392564	0.14860061
\hat{m}_{GDE}			
$m = 0.5$	0.500496858	0.004216106	0.000496858
$m = 1$	0.980884952	0.018350252	-0.019115048
$m = 2$	2.032113782	0.078701255	0.032113782
$m = 5$	5.141084032	0.526581576	0.141084032

the critical values; and the average test statistic D_{avg} values are significantly below the corresponding values. In summary, the K-S test concludes that the two-parameter Gamma PDF can be used to accurately approximate the PDF of Δ .

3.4 Applications and Numerical Results

In this section, we use the Gamma approximate PDF to numerically evaluate the performance of ML-based Nakagami m parameter estimators discussed in Section 3.1 for large N scenarios.

Table 3.2 shows the mean, variance and bias of three ML-based Nakagami m parameter estimators \hat{m}_1 , \hat{m}_2 , and \hat{m}_{GDE} for $m = 0.5, 1, 2$, and 5 with sample size $N = 100$. The numerical results were calculated by using the Gamma approximate PDF of Δ derived in Section 3.3.

By using the relationship

$$\text{MSE}(\hat{m}) = \text{Var}[\hat{m}] + \text{bias}^2(\hat{m}) \quad (3.27)$$

we can evaluate the MSE performance of ML-based m parameter estimators numerically with the data in Table 3.2. Fig. 3.5 shows the simulated MSE of ML-based m parameter estimators discussed in this chapter and the MSE of these m estimators calculated by using the approximate PDF of Δ . The plots show that the calculated MSE values give excellent fit to the simulated MSE curves, which also validates the proposed Gamma approximation. It can be observed in Fig. 3.5 that the Greenwood-Durand estimator \hat{m}_{GDE} and the second order Cheng-Beaulieu estimator \hat{m}_2 achieve very close MSE performance for a variety of fading conditions. In addition, for small and moderate m values ($m < 3$), \hat{m}_{GDE} and \hat{m}_2 perform better than the first order Cheng-Beaulieu estimator \hat{m}_1 in terms of MSE; however, for $m > 3$, which corresponds to less severe fading scenarios, \hat{m}_1 outperforms \hat{m}_{GDE} and \hat{m}_2 .

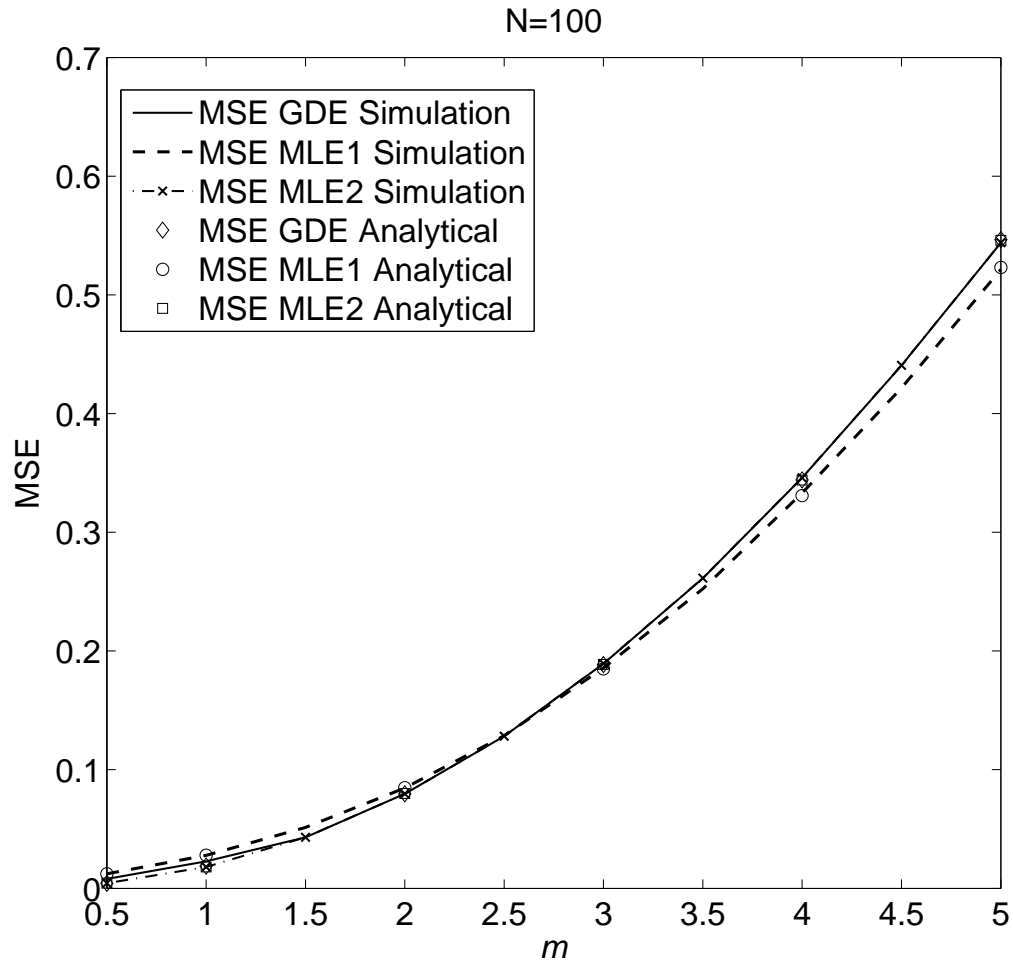


Figure 3.5: Analytical and simulated MSE performance of ML-based Nakagami m parameter estimators with sample size $N = 100$.

3.5 Summary

In this chapter, we have studied statistical properties of a parameter Δ , which is defined as the logarithmic ratio of the arithmetic mean to the geometric mean for the Nakagami- m fading power. This parameter is useful in studying the ML-based estimators of the Nakagami m fading parameter. Closed-form expressions have been derived for both the MGF and the PDF of the parameter Δ . For large sample size, it has been found that the PDF of Δ can be well approximated by a two-parameter Gamma PDF. This approximation has been validated by the Kolmogorov-Smirnov test. As an application, we have applied our results to study the performance of three widely used ML-based Nakagami m parameter estimators.

Chapter 4

Moment-Based Estimation for the Gamma-Gamma Distribution with FSO Applications

4.1 Introduction

Being capable of establishing full-duplex high-speed wireless communication links over a distance of several kilometers using license-free spectrums, free-space optical communication has attracted much attention in the past decade. Because of ease and low cost of implementation, FSO system is considered as an alternative to optical fiber for the 'last mile' problem when fiber optic links are unavailable or too expensive to implement.

As discussed in Chapter 1, in FSO communications the main impairment is caused by atmospheric turbulence-induced irradiance fluctuations. Therefore, when conducting system design and performance analysis for FSO systems, we need to study the atmospheric turbulence models. We reviewed in Chapter 1 that the log-normal distribution [4][5] and the K -distribution [7] were proposed to model the irradiance for weak and strong turbulence conditions respectively. Another turbulence model, the Gamma-Gamma distribution, was later found to be capable of providing good fit to experimental measurements of irradiance for both weak and strong turbulence scenarios [8]. This desirable feature of the Gamma-Gamma distribution enables it to be used in a wide-range of turbulence conditions. The PDF of the Gamma-Gamma distribution is

given by

$$f_G(I) = \frac{2(\alpha\beta)^{(\alpha+\beta)/2}}{\lambda\Gamma(\alpha)\Gamma(\beta)} \left(\frac{I}{\lambda}\right)^{\frac{\alpha+\beta}{2}-1} K_{\alpha-\beta}\left(2\sqrt{\alpha\beta I/\lambda}\right), \quad \alpha > 0, \beta > 0, \lambda > 0 \quad (4.1)$$

where λ is a scale parameter, α and β are the shape parameters, and $K_\nu(\cdot)$ is the ν th order modified Bessel function of the second kind.

To apply turbulence models to the analyses of practical FSO systems, we are often required to estimate the corresponding unknown parameters. Parameter estimation methods for the log-normal distribution and the K -distribution have been well studied in [31] [32] [12] [33]. However, to our best knowledge, estimator for the parameters of the Gamma-Gamma PDF has not been reported in literature. The parameter estimation problem for the Gamma-Gamma distribution is challenging because a maximum-likelihood approach will involve derivatives of $K_\nu(\cdot)$, with respect to both its argument and the order index. For the same reason, the Cramér-Rao lower bound of the estimators can not be easily derived. Current method for determining the shape parameters of the Gamma-Gamma turbulence model has focused on calculating the Rytov variance, which requires the knowledge of link distance and refractive-index structure parameter [31]. However, this requirement is not always desirable for practical FSO systems, especially when terminals have some degrees of portability which can change the link parameters frequently. For FSO systems with slant propagation path, the refractive-index structure parameter can not even be measured accurately because it is a function of altitude, which will change along the slant path.

The remainder of this chapter is organized as follows. Section 4.2 reviews some important statistical properties of the Gamma-Gamma distribution which are useful for our estimation problem. In Section 4.3 we propose an estimation scheme for the Gamma-Gamma turbulence model based on the concept of fractional moments and convex optimization. Then a modified estimator which makes use of the relationship between the Gamma-Gamma shape parameters in FSO applications is proposed in Section 4.4. Simulation results show that significant perfor-

mance improvement in terms of MSE can be achieved by the modified estimation scheme.

4.2 Statistical Properties of the Gamma-Gamma Turbulence Model

4.2.1 Parameterization of the Gamma-Gamma Turbulence Model

Similar to the K -distribution, the Gamma-Gamma turbulence model is developed based on a modulation process, in which small scale irradiance fluctuation is modulated by large scale irradiance fluctuation. In the Gamma-Gamma PDF specified in (4.1), the parameter α represents the effective number of large-scale cells of the scattering process, and the parameter β represents the effective number of small-scale cells [3]. We also emphasize that parameters α and β can not be arbitrarily chosen in FSO applications, they are related through a parameter called Rytov variance, which is a measure of optical turbulence strength. Under an assumption of plane wave and negligible inner scale, which corresponds to long propagation distance and small detector area, the shape parameters of the Gamma-Gamma model satisfy the following relationships [3]

$$\alpha = g(\sigma_R) = \left[\exp \left(\frac{0.49\sigma_R^2}{\left(1 + 1.11\sigma_R^{12/5}\right)^{7/6}} \right) - 1 \right]^{-1} \quad (4.2a)$$

$$\beta = h(\sigma_R) = \left[\exp \left(\frac{0.51\sigma_R^2}{\left(1 + 0.69\sigma_R^{12/5}\right)^{5/6}} \right) - 1 \right]^{-1} \quad (4.2b)$$

where σ_R^2 is the Rytov variance. Though the relationships described in (4.2a) and (4.2b) can change when spherical wave and a finite inner scale are taken into account [8], our estimation approach can be similarly applied to the other scenarios considered in [8]. It can be shown

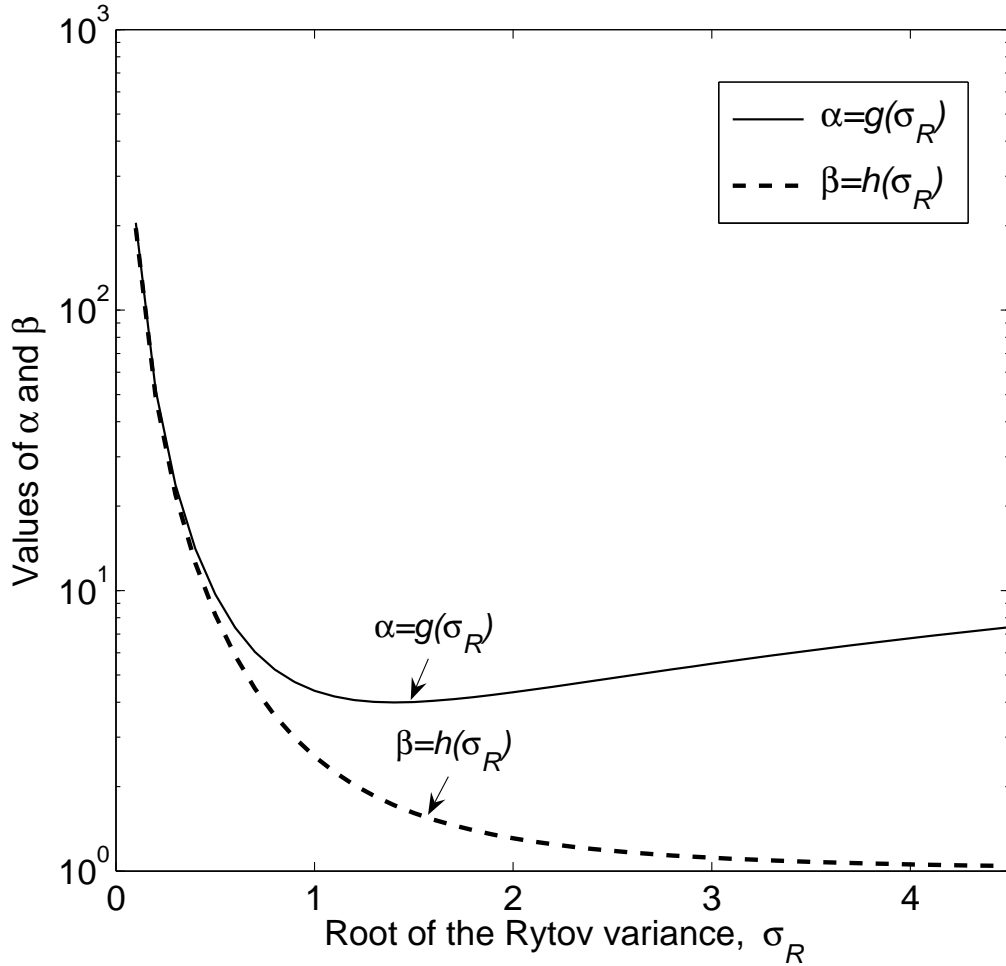


Figure 4.1: Gamma-Gamma shape parameters α and β as functions of σ_R .

that $\alpha = g(\sigma_R)$ in (4.2a) is a convex function of σ_R on $(0, \infty)$, and $\beta = h(\sigma_R)$ in (4.2b) is a monotonically decreasing function on $(0, \infty)$. In addition, the relationship $\alpha > \beta$ always holds, and the smaller shape parameter β is lower bounded above 0.91398 as σ_R approaches infinity. Fig. 4.1 plots α and β as functions of σ_R .

As a measure of optical turbulence strength, the Rytov variance can also be used to characterize different turbulence levels [34]: the weak-turbulence regime refers to $\sigma_R^2 \leq 0.3$; the moderate-turbulence regime has $0.3 < \sigma_R^2 \leq 5$; and the strong-turbulence regime corresponds to $\sigma_R^2 > 5$. However, the definition for fluctuation regimes by the Rytov variance is not strict as

other classification schemes have also been used in literature. For example, in [35] Voelz and Xiao used Rytov variance values between $[1, 10)$ to define the moderate turbulence regime for plane wave scenario. Gamma-Gamma PDFs for weak, moderate, and strong turbulence scenarios are plotted in Fig. 4.2, where the corresponding Rytov variance values are $\sigma_R^2 = 0.25, 2,$ and $11,$ and the scale parameter λ is set to unity. When the Rytov variance σ_R^2 approaches infinity, which corresponds to very severe turbulence condition or the saturation regime, the shape parameter α approaches infinity, the shape parameter β approaches a finite constant $0.91398,$ and the Gamma-Gamma PDF (4.1) will approach a negative exponential PDF. We can observe this trend in Fig. 4.2.

4.2.2 Moments of The Gamma-Gamma Turbulence Model

The k th order moment of the Gamma-Gamma PDF is given by [36]

$$\mu_k = \mathbb{E} [I^k] = \frac{\Gamma(\alpha + k)\Gamma(\beta + k)}{\Gamma(\alpha)\Gamma(\beta)} \left(\frac{\lambda}{\alpha\beta} \right)^k. \quad (4.3)$$

In this work, we normalize the first moment by setting $\lambda = 1.$

The closed-form expression in (4.3) can be derived by applying the following integral property of the modified Bessel function of the second kind (6.561-16, [37]) in the definition of the k th order moment of the Gamma-Gamma distribution

$$\int_0^\infty x^u K_\nu(ax) dx = 2^{u-1} a^{-u-1} \Gamma\left(\frac{1+u+\nu}{2}\right) \Gamma\left(\frac{1+u-\nu}{2}\right), \quad [\Re\{u+1 \pm \nu\} > 0, \Re\{a\} > 0]. \quad (4.4)$$

Note that from the condition of the integral property (4.4), we require

$$\begin{cases} \alpha + k > 0 \\ \beta + k > 0 \end{cases} \quad (4.5)$$

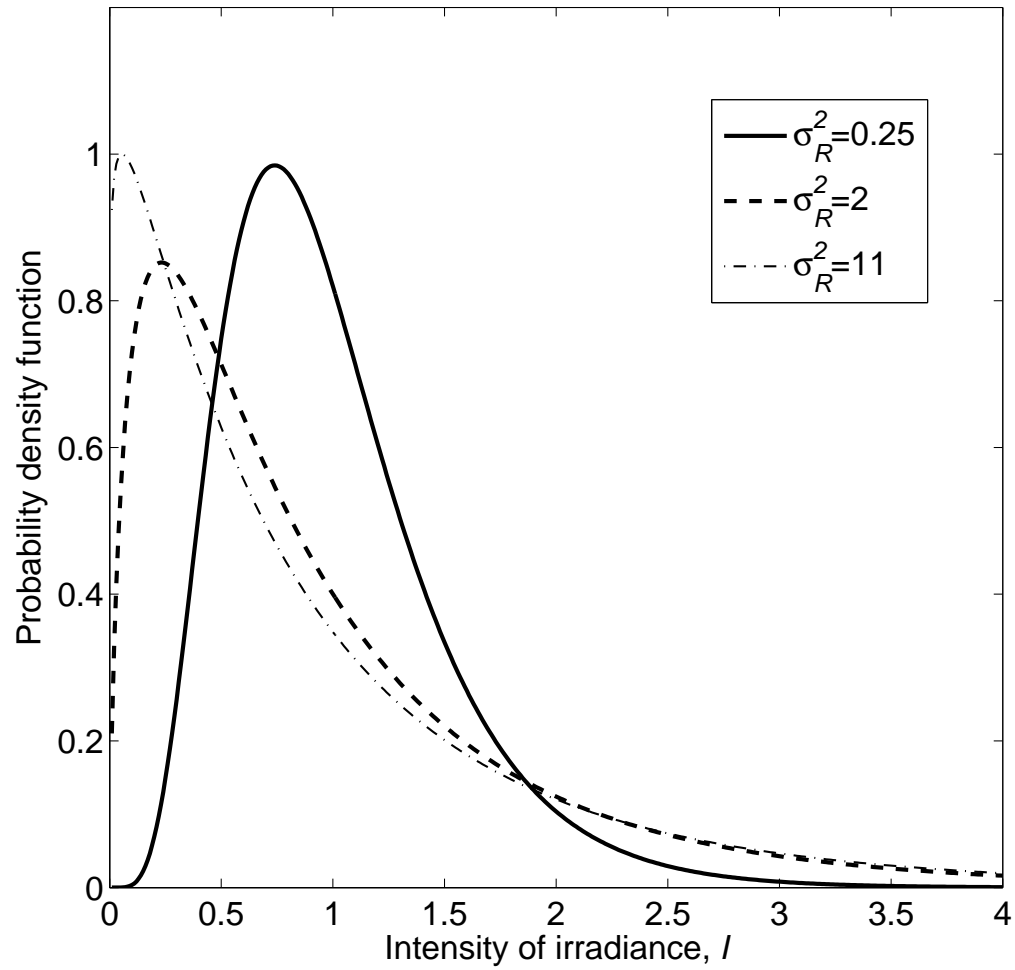


Figure 4.2: Gamma-Gamma PDFs with Rytov variance $\sigma_R^2 = 0.25, 2, \text{ and } 11$.

which means the closed-form moment expression in (4.3) for the Gamma-Gamma distribution is valid only for moments of order greater than $\max\{-\alpha, -\beta\}$. From Section 4.2.1, we know that the minimum of α and β is the limit of β , which is 0.91398. Therefore we conclude the closed-form expression for moments of the Gamma-Gamma distribution in (4.3) is valid for moments of order $k > -0.91398$. Note that the order index k is not restricted to integers, it can also have non-integer values.

4.3 An MoM/CVX Estimation Scheme for Gamma-Gamma Shape Parameters

Taking the ratio of the $(k+1)$ th and the k th order moments of the Gamma-Gamma distribution, we obtain

$$\frac{\mu_{k+1}}{\mu_k} = 1 + \frac{k}{\alpha} + \frac{k}{\beta} + \frac{k^2}{\alpha\beta}. \quad (4.6)$$

From (4.3), we also find that the second-order moment of the Gamma-Gamma distribution is

$$\mu_2 = 1 + \frac{1}{\alpha} + \frac{1}{\beta} + \frac{1}{\alpha\beta}. \quad (4.7)$$

Using (4.6) and (4.7), a nonlinear equation set involving variables α and β is formulated as

$$\begin{cases} \frac{1}{\alpha} + \frac{1}{\beta} = c \\ \frac{1}{\alpha} \cdot \frac{1}{\beta} = d \end{cases} \quad (4.8)$$

where

$$c = \frac{k^2\mu_2 - \frac{\mu_{k+1}}{\mu_k} - (k^2 - 1)}{k^2 - k} \quad (4.9a)$$

$$d = \frac{k\mu_2 - \frac{\mu_{k+1}}{\mu_k} - (k - 1)}{k - k^2}. \quad (4.9b)$$

After some algebraic manipulations to (4.8), α and β values can be found as the roots of the following quadratic equation

$$x^2 - \frac{c}{d}x + \frac{1}{d} = 0. \quad (4.10)$$

For FSO applications, since the shape parameter α is always greater than the shape parameter β , we designate the larger root of (4.10) to be α , and the smaller one to be β . A moment-based shape parameter estimator for the Gamma-Gamma turbulence model can thus be expressed as

$$\hat{\alpha} = \frac{\hat{c}}{2\hat{d}} + \frac{1}{2} \sqrt{\frac{\hat{c}^2}{\hat{d}^2} - \frac{4}{\hat{d}}} \quad (4.11a)$$

$$\hat{\beta} = \frac{\hat{c}}{2\hat{d}} - \frac{1}{2} \sqrt{\frac{\hat{c}^2}{\hat{d}^2} - \frac{4}{\hat{d}}} \quad (4.11b)$$

where \hat{c} and \hat{d} are c and d values in (4.9) calculated using sample moments.

It is known that moment-based estimators with higher order moments may suffer from outlier samples. The outlier problem can be alleviated by choosing smaller k values. To achieve better performance, we propose to use fractional moments ($0 < k < 1$) instead of positive integer moments in our moment-based shape parameter estimators. The application of fractional moments in the study of atmospheric laser scintillation has been discussed by Consortini and Rigal [38]. It has been shown that using fractional moments of orders less than two can significantly reduce the fitting error of moments. Even with the presence of noise and background which can not be removed directly from fractional moments, the fitting accuracy can be guaranteed as long as we have small enough width of the noise of the experimental setup.

Although the denominators of the expressions in (4.9a) and (4.9b) become zero when $k = 0$, it can be shown that the equalities hold for $k = 0$ by applying L'Hôpital's rule as

$$\lim_{k \rightarrow 0} c = \lim_{k \rightarrow 0} \frac{k^2 \mu_2 - \frac{\mu_{k+1}}{\mu_k} - (k^2 - 1)}{k^2 - k} = \lim_{k \rightarrow 0} \frac{2k \mu_2 - \left(\frac{1}{\alpha} + \frac{1}{\beta} + \frac{2k}{\alpha\beta} \right) - 2k}{2k - 1} = \frac{1}{\alpha} + \frac{1}{\beta} \quad (4.12a)$$

$$\lim_{k \rightarrow 0} d = \lim_{k \rightarrow 0} \frac{k\mu_2 - \frac{\mu_{k+1}}{\mu_k} - (k-1)}{k - k^2} = \lim_{k \rightarrow 0} \frac{\mu_2 - \left(\frac{1}{\alpha} + \frac{1}{\beta} + \frac{2k}{\alpha\beta}\right) - 1}{1 - 2k} = \frac{1}{\alpha} \cdot \frac{1}{\beta}. \quad (4.12b)$$

In order to obtain real-valued roots, eqn. (4.10) must have a positive discriminant

$$\Delta = \left(\frac{c}{d}\right)^2 - \frac{4}{d} > 0. \quad (4.13)$$

However, the discriminant Δ may be negative, especially when the Rytov variance becomes small ($\sigma_R < 1$), which corresponds to weak turbulence scenarios. In that case, the moment-based estimator in (4.11) will not give meaningful real-valued estimates for α and β .

To address the above shortcoming, we observe that the left-hand side of (4.10) is a convex function. First, define a function $f(x) = x^2 - \frac{\hat{c}}{d}x + \frac{1}{d}$. Then, a suboptimal solution to the estimation problem can be formulated as a convex optimization problem

$$\begin{aligned} & \underset{\alpha, \beta}{\text{minimize}} && [f(\alpha) - 0]^2 + [f(\beta) - 0]^2 \\ & \text{subject to} && \alpha > 0, \beta > 0. \end{aligned} \quad (4.14)$$

The minimizer for the convex optimization problem described by (4.14) can be found as

$$\hat{\alpha} = \hat{\beta} = \frac{\hat{c}}{2\hat{d}}. \quad (4.15)$$

From Fig. 4.1, it can be seen that when $\sigma_R < 1$, α and β values are close to each other. Thus it is intuitively correct to have suboptimal estimates with $\hat{\alpha} = \hat{\beta}$. By combining the fractional moment-based estimator (4.11) and the convex optimization estimator (4.15), we arrive at a robust estimation scheme for the shape parameters α and β . We name this estimation scheme the method-of-moments/convex-optimization (MoM/CVX) approach.

We use MSE as the metric for assessing the estimation performance. Monte Carlo simula-

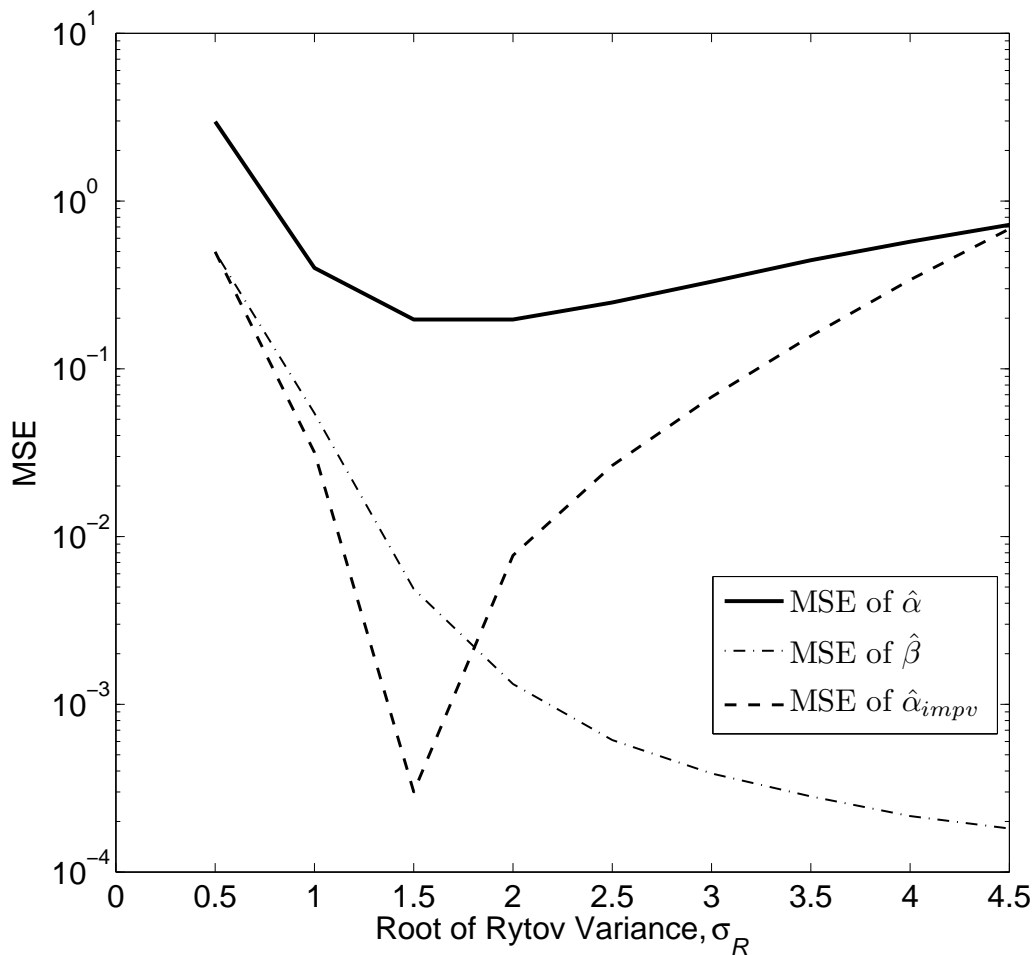


Figure 4.3: MSE performance of the *MoM/CVX* estimator and the modified *MoM/CVX* estimator with $k = 0.5$ and sample size $N = 100,000$.

tions were carried out for the *MoM/CVX* estimator with $k=0.5$ and σ_R value from 0.5 to 4.5, the data sample size was chosen to be $N=100,000$.

From the simulation results shown in Fig. 4.3, we observe that the *MoM/CVX* estimator for β can provide good estimates over a wide range of σ_R values. However, the estimation performance of the *MoM/CVX* estimator for α is poorer. For $\sigma_R = 0.5$, the MSE of $\hat{\alpha}$ can be as large as 2.97, which corresponds to an average relative error of 17.8%. Therefore, we are motivated to further improve the estimation performance for parameter α .

4.4 A Modified MoM/CVX Estimation Scheme for the Shape Parameter α

An alternative method for estimating the shape parameter α , which turns out to be an improved scheme, is to use $\hat{\beta}$ to estimate σ_R via

$$\hat{\sigma}_R = h^{-1}(\hat{\beta}) \quad (4.16)$$

where $h^{-1}(\cdot)$ denotes the inverse function of $h(\cdot)$ in (4.2b). Replacing σ_R in (4.2a) with its estimates in (4.16), a new estimator for α can be obtained as

$$\hat{\alpha}_{impv} = g(h^{-1}(\hat{\beta})). \quad (4.17)$$

The analytical expression of $h^{-1}(\cdot)$ is cumbersome; however, the built-in function `solve` in MATLAB can be used to find numerical results for $h^{-1}(\cdot)$.

We observe in Fig. 4.3 that the MSE performance of the estimates of α is significantly improved by the modified method (dashed line). For our sample points, the largest improvement is achieved at $\sigma_R = 1.5$, where the MSE is reduced by 99.85%.

The change in improvement achieved by the modified scheme can actually be predicted. For example, from a plot of $|g'(\sigma_R)|$ versus σ_R shown in Fig. 4.4, one obtains $|g'(\sigma_R)| = 0$ when $\sigma_R = 1.402567471$. This suggests that the modified estimator $\hat{\alpha}_{impv}$ is least sensitive to the estimation error of $\hat{\beta}$ in the neighborhood of this point and the largest improvement for estimates of α can be achieved.

Fig. 4.5 summarizes the estimation process of the modified MoM/CVX estimator. In the modified estimation scheme, we first calculate sample moments $\hat{\mu}_k$, $\hat{\mu}_{k+1}$ and $\hat{\mu}_2$ of the Gamma-Gamma turbulence model from the observed optical irradiance sample values. Parameters \hat{c} and \hat{d} in (4.9) can then be determined by using the sample moments. If the discriminant Δ of

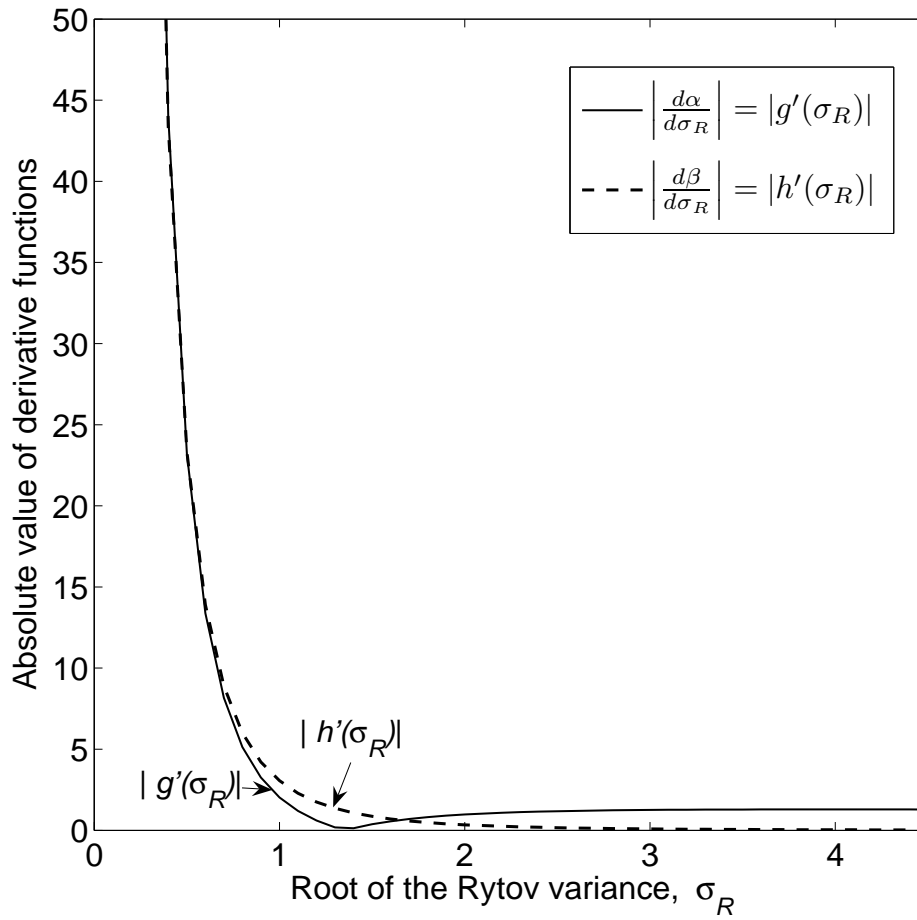


Figure 4.4: Absolute derivative functions of the Gamma-Gamma shape parameters α and β with respect to σ_R .

the quadratic equation in (4.10) is greater than zero, we use the quadratic solution in (4.11) to obtain the estimate of parameter β ; otherwise, an estimate of β will be given by the convex optimization solution (4.15). With an estimate of β , we can finally find an improved estimator $\hat{\alpha}_{impv}$ via (4.17).

4.5 Summary

In this chapter, we have studied the parameter estimation problem for the Gamma-Gamma turbulence model for free-space optical communications. An estimation scheme for the shape parameters of the Gamma-Gamma distribution has been proposed based on the concept of fractional moments and convex optimization. With the proposed method, estimates of the shape parameters can be directly obtained from observed samples, which is more straightforward than the current method which depends on measurements of some physical quantities. To improve the estimation performance, we have also proposed a modified scheme which exploits the relationship between the Gamma-Gamma shape parameters in FSO communications. Simulation results have revealed that the modified estimation scheme can achieve MSE below 0.5 and average relative estimation error below 15% for a wide range of turbulence conditions and system setups.

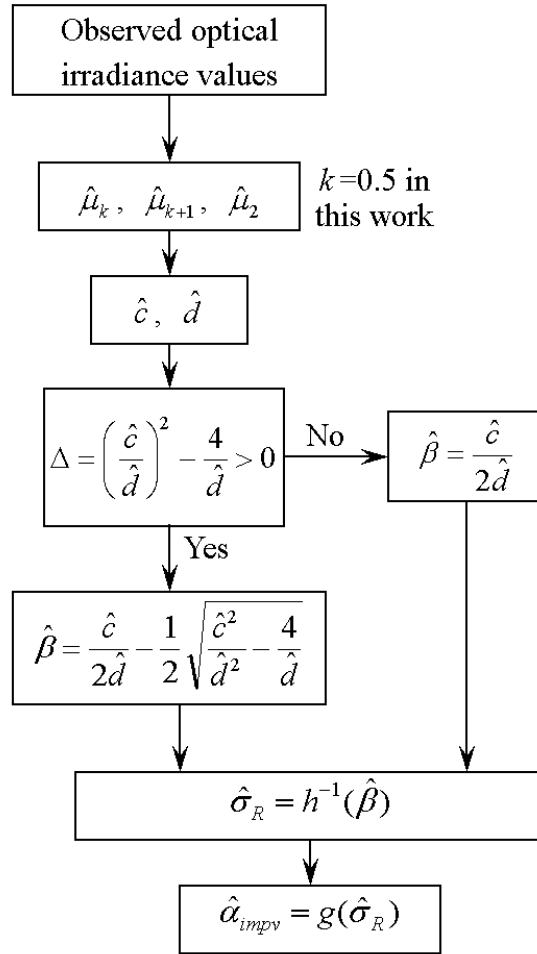


Figure 4.5: Flow chart of the modified *MoM/CVX* estimator for the Gamma-Gamma shape parameters.

Chapter 5

Conclusions

This chapter concludes the thesis with some general comments on applications of the method of moments on parameter estimation for fading and atmospheric models in wireless communication, followed by a discussion of possible future work for investigation of alternative applicable estimation methods and applications.

5.1 Summary of Contributions

In this thesis, we have investigated applications of several moment-based methods in parameter estimation of fading and atmospheric turbulence models. The contributions of this thesis can be summarized as follows.

1. A detailed discussion on moment-based estimation for the Nakagami- m fading model has been given. A family of classical moment-based m parameter estimators has been reviewed. Both the integer moments scenario and the fractional moments scenario are discussed. The generalized method of moment estimation which exploits information that resides in all available moment conditions in a determined or over-determined estimation problem, has been introduced to fading parameter estimation for the first time. Systematic performance comparison for moment-based m parameter estimators has been conducted by both simulation and an analytical asymptotic variance analysis.
2. By investigating the statistical properties of the parameter Δ , which is defined as the logarithmic ratio of the arithmetic mean to geometric mean for the Nakagami- m fading

power, the MGF and the exact PDF of Δ have been derived. A Gamma approximation of the PDF of Δ , which avoids computational complexity of the exact PDF for large sample size, has also been proposed by using a moment matching method. The validity of using the two-parameter Gamma PDF to approximate the PDF of Δ has been established using the Kolmogorov-Smirnov test. With the assistance of our results, numerical evaluation of the performance of ML-based Nakagami m parameter estimators is feasible without performing intensive Monte Carlo simulations.

3. Based on the concepts of fractional moments and convex optimization, we have proposed a composite estimation scheme for the shape parameters of the Gamma-Gamma atmospheric turbulence model. Our estimation technique can be used to characterize this atmospheric turbulence model over a wide range of turbulence conditions in FSO applications.

5.2 Future work

The GMM approach introduced in Section 2.3 provides a general framework for an iterative estimation scheme based on moment conditions. It has been shown that the GMM approach can achieve very good estimation performance for Nakagami m parameter estimation, and under this framework, using more moment conditions can further improve the estimation performance. Therefore, when the computation load is affordable and the delay requirement is not strict, it is preferable to use the GMM in any estimation problem in wireless communication research like the Gamma-Gamma estimation problem discussed in Chapter 4 and channel estimation etc. to improve moment-based estimation accuracy. Particularly, this GMM approach has large potential application in wireless communication problems where the traditional ML-based estimation approach does not work.

Another possible future research topic is the application of the L-moment method men-

tioned in Section 1.3. Most moment-based estimation schemes require the sample size to be very large to guarantee the convergence of the sample moments. However, for many real-time applications, this requirement can not be satisfied. The L-moments, being linear combinations of data, are less influenced by outliers and suffer less from sampling variability. Therefore, the L-moment method may be preferred in such real-time scenarios to the ML approach when ML has high computational complexity.

Bibliography

- [1] D. Tse and P. Viswanath, *Fundamentals of Wireless Communication*. Cambridge: Cambridge University Press, 2005.
- [2] M. Nakagami, “The m -distribution as a general formula of intensity distribution of rapid fading,” *Statistical Methods in Radio Wave Propagation*, vol. 40, pp. 757–768, Nov. 1962.
- [3] L. C. Andrews, R. L. Phillips, and C. Y. Hopen, *Laser Beam Scintillation with Applications*. Bellingham, WA: SPIE Press, 2001.
- [4] G. Parry, “Measurements of atmospheric turbulence-induced intensity fluctuations in a laser beam,” *Optica Acta*, vol. 28, no. 5, pp. 715–728, May 1981.
- [5] R. L. Phillips and L. C. Andrews, “Measured statistics of laser-light scattering in atmospheric turbulence,” *Journal of the Optical Society of America*, vol. 71, no. 12, pp. 1440–1445, Dec. 1981.
- [6] J. H. Churnside and R. G. Frehlich, “Experimental evaluation of lognormally modulated Rician and IK models of optical scintillation in the atmosphere,” *Journal of the Optical Society of America. Series A*, vol. 6, no. 11, pp. 1760–1766, Nov. 1989.
- [7] E. Jakeman and P. N. Pusey, “The significance of K -distributions in scattering experiments,” *Physics Review Letters*, vol. 40, no. 9, pp. 546–550, Sept. 1978.

- [8] M. A. Al-Habash, L. C. Andrews, and R. L. Phillips, “Mathematical model for the irradiance probability density function of a laser beam propagating through turbulent media,” *Optical Engineering*, vol. 40, no. 8, pp. 1554–1562, Aug. 2001.
- [9] S. M. Kay, *Fundamentals of Statistical Signal Processing: Estimation Theory*. Upper Saddle River, NJ: Prentice Hall, 1993.
- [10] L. P. Hansen, “Large sample properties of generalized method of moments estimators,” *Econometrica*, vol. 50, no. 4, pp. 1029–1054, July 1982.
- [11] J. R. M. Hosking, “L-moments: Analysis and estimation of distributions using linear combinations of order statistics,” *Journal of the Royal Statistical Society. Series B*, vol. 52, no. 1, pp. 105–124, Jan. 1990.
- [12] D. R. Iskander, A. M. Zoubir, and B. Boashash, “A method for estimating the parameters of the K -distribution,” *IEEE Transactions on Signal Processing*, vol. 47, no. 4, pp. 1147–1151, Apr. 1999.
- [13] M. Hadžialić, M. Milišić, N. Hadžiahmetović, and A. Sarajlić, “Moment-based and maximum likelihood-based quotiential estimation of the Nakagami- m fading parameter,” in *Proc. IEEE Vehicular Technology Conference, VTC2007-Spring*, Dublin, Ireland, Apr. 22-25, 2007, pp. 549–553.
- [14] G. Yin, “Bayesian generalized method of moments,” *Bayesian Analysis*, vol. 4, no. 2, pp. 191–208, Feb. 2009.
- [15] J. A. Greenwood and D. Durand, “Aids for fitting the gamma distribution by maximum likelihood,” *Technometrics*, vol. 2, no. 1, pp. 55–64, Feb. 1960.
- [16] J. Cheng and N. Beaulieu, “Maximum-likelihood based estimation of the Nakagami m parameter,” *IEEE Communications Letters*, vol. 5, pp. 101–103, Mar. 2001.

- [17] A. Abdi and M. Kaveh, “Performance comparison of three different estimators for the Nakagami m parameter using monte carlo simulation,” *IEEE Communications Letters*, vol. 4, no. 4, pp. 119–121, Apr. 2000.
- [18] V. Barnett and T. Lewis, *Outliers in Statistical Data*, 3rd ed. Chichester, NY: John Wiley & Sons, 1994.
- [19] J. Cheng and N. Beaulieu, “Generalized moment estimators for the Nakagami fading parameters,” *IEEE Communications Letters*, vol. 6, pp. 144–146, Apr. 2002.
- [20] J. Cheng, *Performance Analysis of Digital Communications Systems with Fading and Interference*, Ph.D. thesis, University of Alberta, Edmonton, A.B., Canada, Dec. 2002.
- [21] E. L. Lehmann, *Elements of Large-Sample Theory*. New York: Springer-Verlag, 1999.
- [22] M. S. Bartlett, *An Introduction to Stochastic Processes*, 3rd ed. Cambridge: Cambridge University Press, 1978.
- [23] Q. T. Zhang, “A note on the estimation of Nakagami- m fading parameter,” *IEEE Communications Letters*, vol. 6, no. 6, pp. 237–238, June 2002.
- [24] H. C. Thom, “A note on the Gamma distribution,” *Monthly Weather Review*, vol. 86, no. 4, pp. 117–122, Apr. 1958.
- [25] R. V. Hogg and A. T. Craig, *Introduction to Mathematical Statistics*, 5th ed. Upper Saddle River, NJ: Prentice Hall, 1995.
- [26] P. Bullen, *Handbook of Means and Their Inequalities*, 2nd ed. New York: Springer, 1987.
- [27] G. A. Gibson, *Advanced Calculus*. London: Macmillan, 1931.
- [28] E. T. Whittaker and G. N. Watson, *A Course of Modern Analysis*, 4th ed. Cambridge: Cambridge University Press, 1962.

- [29] A. M. Mathai and R. K. Saxena, *Generalized Hypergeometric Functions With Applications In Statistics And Physical Sciences*. New York: Springer-Verlag, 1973.
- [30] A. H.-S. Ang and W. H. Tang, *Probability Concepts in Engineering*, 2nd ed. Hoboken, NJ: John Wiley & Sons, 2007.
- [31] A. C. Cohen Jr., “Estimating parameters of logarithmic-normal distributions by maximum likelihood,” *Journal of the American Statistical Association*, vol. 46, no. 254, pp. 206–212, June 1951.
- [32] A. H. Munro and R. A. J. Wixley, “Estimators based on order statistics of small samples from a three-parameter lognormal distribution,” *Journal of the American Statistical Association*, vol. 65, no. 329, pp. 212–225, Mar. 1970.
- [33] I. R. Joughin, D. B. Percival, and D. Winebrenner, “Maximum likelihood estimation of K distribution parameters for SAR data,” *IEEE Transactions on Geoscience and Remote Sensing*, vol. 31, no. 5, pp. 989–999, Sept. 1993.
- [34] A. Prokeš, “Modeling of atmospheric turbulence effect on terrestrial FSO link,” *Radio Engineering*, vol. 18, no. 1, pp. 42–47, Apr. 2009.
- [35] D. G. Voelz and X. Xiao, “Metric for optimizing spatially partially coherent beams for propagation through turbulence,” *Optical Engineering*, vol. 48, no. 3, pp. 036001–036001–7, Mar. 2009.
- [36] W. Gappmair and S. S. Muhammad, “Error performance of PPM/Poisson channels in turbulent atmosphere with gamma-gamma distribution,” *Electronics Letters*, vol. 43, no. 16, pp. 880–882, Aug. 2007.
- [37] I. S. Gradshteyn and I. M. Ryzhik, *Table of Integrals, Series, and Products*, 7th ed. London: Academic Press, 2007.

- [38] A. Consortini and F. Rigal, “Fractional moments and their usefulness in atmospheric laser scintillation,” *Pure and Applied Optics*, vol. 7, no. 5, pp. 1013–1032, May 1998.
- [39] H. V. Poor, *An Introduction to Signal Detection and Estimation*, 2nd ed. New York: Springer, 1994.

Appendix A

Derivation of (2.28)

By taking partial derivatives of $h(\hat{m}_{GMM}; \hat{\mu}_{k1}, \dots, \hat{\mu}_{ks})$ in (2.27) and setting $\hat{\mu}_{k1} = \mu_{k1}, \dots, \hat{\mu}_{ks} = \mu_{ks}$, we have

$$\begin{aligned} & \left. \frac{\partial h(\hat{m}_{GMM}; \hat{\mu}_{k1}, \dots, \hat{\mu}_{ks})}{\partial \hat{m}_{GMM}} \right|_{\hat{\mu}_{k1}=\mu_{k1}, \dots, \hat{\mu}_{ks}=\mu_{ks}} \\ &= -2 \left(\left. \frac{\partial \mu_{k1}}{\partial m} \right|_{m=\hat{m}_{GMM}}, \dots, \left. \frac{\partial \mu_{ks}}{\partial m} \right|_{m=\hat{m}_{GMM}} \right) \Sigma^{-1} \begin{pmatrix} \left. \frac{\partial \mu_{k1}}{\partial m} \right|_{m=\hat{m}_{GMM}} \\ \vdots \\ \left. \frac{\partial \mu_{ks}}{\partial m} \right|_{m=\hat{m}_{GMM}} \end{pmatrix} \end{aligned} \quad (\text{A.1a})$$

$$\begin{aligned} & \left(\left. \frac{\partial h(\hat{m}_{GMM}; \hat{\mu}_{k1}, \dots, \hat{\mu}_{ks})}{\partial \hat{\mu}_{k1}}, \dots, \left. \frac{\partial h(\hat{m}_{GMM}; \hat{\mu}_{k1}, \dots, \hat{\mu}_{ks})}{\partial \hat{\mu}_{ks}} \right) \right) \Big|_{\hat{\mu}_{k1}=\mu_{k1}, \dots, \hat{\mu}_{ks}=\mu_{ks}} \\ &= -2 \left(\left. \frac{\partial \mu_{k1}}{\partial m} \right|_{m=\hat{m}_{GMM}}, \dots, \left. \frac{\partial \mu_{ks}}{\partial m} \right|_{m=\hat{m}_{GMM}} \right) \Sigma^{-1} \begin{pmatrix} 1 & 0 & \dots & 0 \\ 0 & 1 & \dots & 0 \\ \vdots & \vdots & \ddots & \vdots \\ 0 & 0 & \dots & 1 \end{pmatrix}_{ks \times ks}. \end{aligned} \quad (\text{A.1b})$$

Denoting

$$\eta = \left(\left. \frac{\partial \mu_{k1}}{\partial m} \right|_{m=\hat{m}_{GMM}}, \dots, \left. \frac{\partial \mu_{ks}}{\partial m} \right|_{m=\hat{m}_{GMM}} \right) \Sigma^{-1} \begin{pmatrix} \left. \frac{\partial \mu_{k1}}{\partial m} \right|_{m=\hat{m}_{GMM}} \\ \vdots \\ \left. \frac{\partial \mu_{ks}}{\partial m} \right|_{m=\hat{m}_{GMM}} \end{pmatrix} \quad (\text{A.2})$$

and substituting (A.1) and (2.27) into (2.25), we arrive at

$$\begin{aligned}
 \sigma_{GMM}^2 &= \frac{1}{\eta^2} \left(\frac{\partial \mu_{k1}}{\partial m} \Big|_{m=\hat{m}_{GMM}}, \dots, \frac{\partial \mu_{ks}}{\partial m} \Big|_{m=\hat{m}_{GMM}} \right) \Sigma^{-1} \Sigma \Sigma^{-1} \begin{pmatrix} \frac{\partial \mu_{k1}}{\partial m} \Big|_{m=\hat{m}_{GMM}} \\ \vdots \\ \frac{\partial \mu_{ks}}{\partial m} \Big|_{m=\hat{m}_{GMM}} \end{pmatrix} \\
 &= \frac{1}{\eta^2} \left(\frac{\partial \mu_{k1}}{\partial m} \Big|_{m=\hat{m}_{GMM}}, \dots, \frac{\partial \mu_{ks}}{\partial m} \Big|_{m=\hat{m}_{GMM}} \right) \Sigma^{-1} \begin{pmatrix} \frac{\partial \mu_{k1}}{\partial m} \Big|_{m=\hat{m}_{GMM}} \\ \vdots \\ \frac{\partial \mu_{ks}}{\partial m} \Big|_{m=\hat{m}_{GMM}} \end{pmatrix} \quad (\text{A.3}) \\
 &= \left[\left(\frac{\partial \mu_{k1}}{\partial m} \Big|_{m=\hat{m}_{GMM}}, \dots, \frac{\partial \mu_{ks}}{\partial m} \Big|_{m=\hat{m}_{GMM}} \right) \Sigma^{-1} \begin{pmatrix} \frac{\partial \mu_{k1}}{\partial m} \Big|_{m=\hat{m}_{GMM}} \\ \vdots \\ \frac{\partial \mu_{ks}}{\partial m} \Big|_{m=\hat{m}_{GMM}} \end{pmatrix} \right]^{-1} = \frac{1}{\eta}.
 \end{aligned}$$

Appendix B

Exponential Family Property of the Nakagami- m Distribution

An s -parameter exponential family is defined as a family of distributions parameterized by an s -dimensional vector $\theta = [\theta_1, \theta_2, \dots, \theta_s]^T$ with PDF in the form of

$$f_X(x; \theta) = C(\theta) \exp \left\{ \sum_{i=1}^s \eta_i(\theta) \mathbf{T}_i(\mathbf{x}) \right\} h(\mathbf{x}) \quad (\text{B.1})$$

where C , η_i 's are real-valued functions of θ , and T_i s and h are real-valued functions of x [39]. If N *i.i.d.* random samples X_1, X_2, \dots, X_N are drawn according to an exponential family distribution with PDF in the form of (B.1), then $(\sum_{i=1}^N T_j(X_i), j = 1, 2, \dots, s)$ is a joint complete sufficient statistic.

We rewrite the PDF of the Nakagami- m distribution (3.1) as

$$\begin{aligned} f_R(r; m, \Omega) &= \frac{2}{\Gamma(m)} \left(\frac{m}{\Omega}\right)^m r^{2m-1} \exp \left\{ -\frac{m}{\Omega} r^2 \right\} \\ &= \frac{2}{\Gamma(m)} \left(\frac{m}{\Omega}\right)^m \exp \left\{ \ln r^{2m} \right\} \frac{1}{r} \exp \left\{ -\frac{m}{\Omega} r^2 \right\} \\ &= \frac{2}{\Gamma(m)} \left(\frac{m}{\Omega}\right)^m \exp \left\{ -\frac{m}{\Omega} r^2 + m \ln r^2 \right\} \frac{1}{r}. \end{aligned} \quad (\text{B.2})$$

If we denote $C(m, \Omega) = \frac{2}{\Gamma(m)} \left(\frac{m}{\Omega}\right)^m$, $\eta_1(m, \Omega) = -m/\Omega$, $\eta_2(m, \Omega) = m$, $T_1(r) = r^2$, $T_2(r) = \ln r^2$, and $h(r) = 1/r$, then the Nakagami- m PDF can fit in the form of (B.1), which suggests that the Nakagami- m distribution is a member of a two-parameter exponential family.

Thus $(\sum_{i=1}^N R_i^2, \sum_{i=1}^N \ln R_i^2) = (\sum_{i=1}^N T_1(R_i), \sum_{i=1}^N T_2(R_i))$ is a joint complete sufficient statis-

tics of the Nakagami- m distribution. Therefore, the parameter Δ , which can be written as

$$\begin{aligned}\Delta &= \ln \left(\frac{1}{N} \sum_{i=1}^N R_i^2 \right) - \ln \left[\left(\prod_{i=1}^N R_i^2 \right)^{\frac{1}{N}} \right] \\ &= \ln \left(\frac{1}{N} \sum_{i=1}^N T_1(R_i) \right) - \frac{1}{N} \sum_{i=1}^N T_2(R_i)\end{aligned}\tag{B.3}$$

is a function of the joint complete sufficient statistics of the Nakagami- m distribution.